



Live Webinar Series: From Polar Pesticide Panels to Multiresidue Mega-Methods

This scientific eSeminar Series addresses pesticide analysis in food for panels of polar pesticides and how to successfully implement 'mega' methods for hundreds of residues, whilst adhering to the latest SANTE/ 11312/2021 guidelines.

Quantitative Analysis of 764 Pesticides in Tomato by LC/MS/MS

Tuesday, 06 June 2023, 3:00 p.m. CEST

A Robust Method For the Sensitive Analysis of Non-Derivatized Polar Pesticides in Food by LC/MS/MS

Wednesday, 14 June 2023, 3:00 p.m. CEST



See abstracts
and register!

On optimum dynamic temperature profiles for thermal inactivation kinetics determination

Maria C. Giannakourou¹  | Konstantinos-Philip Saltaouras² |
Nikolaos G. Stoforos² 

¹ Department of Food Science and Technology, University of West Attica, Athens, Greece

² Department of Food Science and Human Nutrition, Agricultural University of Athens, Athens, Greece

Correspondence

Nikolaos G. Stoforos, Department of Food Science and Human Nutrition, Agricultural University of Athens, Athens 11855, Greece.

Email: stoforos@aua.gr

Abstract: Determination of inactivation kinetics, associated with thermal processing of foods and obtained from dynamic temperature experiments, requires carefully designed experiments, the primary element being the selection of the appropriate temperature profile along with a carefully planned sampling schedule. In the present work, a number of different dynamic temperature profiles were investigated in terms of their ability to generate accurate kinetic parameters with low confidence intervals (CIs). Although alternative models have been also tested, our work was concentrated on thermal inactivation kinetics that could be described by the classical D - z values. A pair of D and z values was assumed, and for each temperature profile tested, concentration data at different processing times were generated through the appropriate models. Next, an error (up to $\pm 2.5\%$ or $\pm 5\%$) was introduced on these theoretical values to generate pseudo-experimental data, and the back-calculation of the assumed kinetic parameters by non-linear regression was performed. The accuracy and the 95% CIs of the estimated kinetic parameters were evaluated; joint confidence regions were also constructed to investigate parameters correlation. The effect of temperature profile pattern, level of error, number of experimental points, and reference temperature was assessed. A stepwise increasing and a single triangle-pattern temperature profile were the best profiles among those tested. As a general observation, based on different kinetic models investigated, temperature profiles and sampling intervals that result in concentration versus time diagrams having shapes as suggested by the primary model used when isothermally applied are not considered appropriate for parameter estimation.

Nomenclature: b , regression coefficient appearing in in Equations (4) and (5); b_1 , regression coefficient appearing in Weibull-type model (Equation 16); C , concentration of a heat-labile substance, number of microorganisms/mL, spores per container, g/mL, or any other appropriate unit; D_T , decimal reduction time or death rate constant–time at a constant temperature required to reduce by 90% the initial spore load (or, in general, the time required for 90% reduction of a heat-labile substance), min; $F(p, n-p, 1-a)$, the upper $1-a$ quantile for an F-distribution with p and $n-p$ degrees of freedom; k , slope of Equation (17), (Weibull-type model) min^{-1} ; J , Jacobian matrix; n , number of observations; n_1 , coefficient in Weibull-type model (Equation 16); p , number of estimated parameters; r , correlation coefficient (Equation 12); $RMSE$, root mean square error (Equation 15); S , survival ratio; SE , standard error of each parameter; SSE , sum of squared errors; T , (product) temperature ($^{\circ}\text{C}$); t , time (min); z , temperature difference required to achieve a decimal change of the D_T value ($^{\circ}\text{C}$); Subscripts: i , for i equals 1 to n , referring to the i^{th} experimental point; c , temperature index in the Weibull-type model (Equation 17); ref , reference value; o , initial condition; obs , observed (experimental point); $pred$, predicted (mathematically estimated through equations); T , temperature; Superscripts: T , matrix/vector transpose operator (Equation 7).

KEYWORDS

time-varying temperature, thermal inactivation, modeling, parameter estimation, simulation, uncertainty, joint confidence intervals

1 | INTRODUCTION

Modeling the inactivation of microorganisms, enzymes, and other heat-labile indices is essential for assessing the efficiency of preservation processes that are designed to reduce their population density, activity, or concentration (Fleischman, 2015) and thus for describing and predicting the quality and the safety of processed foods (Mastwijk et al., 2017). To carry out a systematic kinetic study, different methodologies have been used in current literature, with the majority of them being based mainly on experiments under isothermal conditions (Goula et al., 2018).

In this context, the determination of thermal inactivation kinetic parameters of a safety or quality attribute is traditionally accomplished through a two-step procedure, from data collected during constant temperature experiments. Thus, in a first step, inactivation rates at selected constant temperatures are evaluated through remaining concentration measurements of the particular heat-labile agent under investigation at different processing times through an appropriate primary model; the purpose of this stage is to calculate the reaction rate constant k or, equivalently, any other appropriate parameter. In a second step, the temperature dependence of the selected parameter used to describe the inactivation rate, calculated in the first step, is described through the use of a particular secondary model. While Arrhenius-type equations are the most popular secondary models applied to illustrate the temperature dependence of chemical and biochemical reactions, in an alternative thermobacteriological approach, the temperature dependence of the decimal reduction time, the D value, is expressed with the z -value, defined as the increase in temperature necessary to induce a 10-fold reduction in D value. There are numerous recently published isothermal studies that aimed at calculating the D and z -values, either in the case of microbial (Huang, 2013; Juneja et al., 2001; Murphy et al., 2003; Wang et al., 2017) or of enzyme inactivation (Aghajanzadeh et al., 2016; Cao et al., 2018; Cheng et al., 2013; He et al., 2017). The typical analysis of the data during the two-step approach is easily implemented. However, the kinetic parameters of the secondary model are derived from estimates of the primary model, which are already characterized by an estimation error that is not necessarily taken into account (Giannakourou & Stoforos, 2017; Van Derlinden & Van Impe, 2012). Alternatively, from the same data at isothermal conditions, model parameters can be determined in a single step, considering the dataset as a whole, by incorporating the secondary model equa-

tions into the primary model and performing a non-linear regression (Conesa et al., 2003). This allows for the estimation of kinetic parameters with narrower confidence intervals (CIs), compared to the two-step data analysis, due to the increased number of degrees of freedom (Van Boekel, 1996).

One should notice, however, that caution is needed when applying inactivation model equations and their associated kinetic parameters obtained under isothermal conditions to dynamic profiles, as this projection may lead to serious errors in the obtained predictions (Dolan, 2003; Valdramidis et al., 2006). According to Gil et al. (2006), the kinetic parameters estimated under non-isothermal conditions may differ from the ones predicted at constant temperatures, and this may cause a significant prediction error. A way to overcome this pitfall is by estimating parameters directly through experiments under dynamic temperature profiles, close to real processing conditions (Vieira et al., 2002). In this context, both primary and secondary model kinetic parameters can be evaluated in one step through remaining concentration versus time data from a single experiment at time-varying temperature conditions. It should be stressed out, however, that calculating the inactivation parameters from dynamic temperature data requires more complicated numerical algorithms instead of standard non-linear regression techniques (Corradini et al., 2008). Several studies, in the recent literature, have demonstrated the advantages of estimating kinetic parameters using non-isothermal temperature conditions either during inactivation (Cattani et al., 2016; Corradini et al., 2005; Goula et al., 2018; Greiby et al., 2017; Huang, 2013; Kubo et al., 2018; Valdramidis et al., 2008) or microbial growth (Cornet et al., 2010; Huang, 2016; Huang & Vinyard, 2016; Longhi et al., 2017; Van Derlinden et al., 2008).

At the early stages, researchers used temperature profiles, as functions of time, $T(t)$, such as linear, exponential, and so forth, (Cunha & Oliveira, 2000; Hayakawa et al., 1969; Leontidis et al., 1999; Nunes et al., 1991; Rhim et al., 1989a, 1989b) that led to analytical solutions of concentration versus time equations. The potential effect of the form of the selected temperature profile on the accuracy and reliability of parameters estimation was studied in Van Derlinden and Van Impe (2010, 2012), Versyck et al. (1999) and Versyck et al. (2000). In the majority of the studies for inactivation kinetics, first-order kinetics were assumed, although there are several publications where

other models (Weibull, log-logistic, reparametrized Gompertz equation, etc.) have been selected to describe inactivation data under dynamic conditions in order to account for the observed non-linearity (Aragao et al., 2007; Corradini et al., 2006; Corradini & Peleg, 2007; Huang, 2009; Mastwijk et al., 2017; Peleg et al., 2001; Peleg et al., 2008; Timmermans et al., 2017; Valdramidis et al., 2008; Van Boekel, 2002).

In the works of Van Derlinden and Van Impe (2010, 2012), Versyck et al. (1999) and Versyck et al. (2000), the approach of optimal experimental design was introduced, and its main concepts were outlined. D-optimality condition maximizes the determinant $\det(J^T \cdot J)$, for J being the Jacobian matrix with the partial derivatives of the model output with respect to the model parameters evaluated at each measurement point and leads to minimum estimation errors on the parameters (Grijpspeerdt, & De Reu, 2005, John, & Draper, 1975). Van Derlinden and Van Impe (2010, 2012) studied the effect of the form of the selected temperature profile on the accuracy and reliability of parameters estimation based on the D-optimality condition. A similar approach was used by Versyck et al. (1999) and Versyck et al. (2000), where the focus was drawn on the optimization of time-temperature profiles with respect to Fischer information matrix-based objective functions in order to estimate the kinetic parameters of thermal inactivation. The Fisher information matrix is the inverse of the error covariance matrix of the best linear unbiased estimators; it provides information concerning the measurement errors and parameter sensitivities, allowing for the evaluation of the quality of parameter estimation (Munack, 1989; Versyck et al., 1999;). Representative step profiles were analyzed through a simulation procedure, and the resulting joint confidence contour plots were constructed. The initial guesses for the kinetic parameters $D_{T_{ref}}$ and z -value were obtained from data from isothermal studies.

An important issue related to parameter estimation refers to the reporting of the uncertainty of kinetic parameters via the calculation of their CIs. Dolan (2003) points out that there may be more than one combination of parameters that give identical results, and that it is essential to calculate CIs in order to assess the uncertainty of the parameters. In the majority of published studies concerning the estimation of $D_{T_{ref}}$ and z -values for inactivation kinetics, the 95% CIs of each parameter were separately calculated, either based on the least squares regression analysis (in the case of isothermal studies) and/or by an appropriate statistical package, based on t -test statistics and the covariance matrix (e.g., MATLAB, in the case of non-isothermal conditions), and results are reported as the mean estimate $\pm 95\%$ CI (Cattani et al., 2016; Conesa et al., 2003; Dolan, 2003; Garre et al., 2018; Garre et al., 2017). When

applying methodologies of simultaneous estimation of all kinetic parameters (based either on isothermal or time-varying experiments), one cannot overlook their potential correlation, which means that the CI of each parameter depends on the value of the other parameters involved (Goula et al., 2018). For these cases, the quality of the simultaneously estimated model parameters is assessed by the construction of the joint confidence regions of the parameters involved (Bernaerts et al., 2000; Claeys et al., 2001; Dolan et al., 2007; Bernaerts et al., 2002; Fernández et al., 2001; Fernández et al., 1999; Haralampu et al., 1985; Valdramidis et al., 2008; Dolan et al., 2015).

In summary, recent research has been focused on calculating kinetic parameters from dynamic temperature experiments. However, no universal, standardized approach has been used as far as kinetic parameter estimation is concerned. In terms of time-temperature profiles employed, the majority of the works use combinations of exponentially or linearly increasing and constant temperature segments. Rarely different time-temperature profiles are compared or evaluated in terms of the accuracy and confidence with which the kinetic parameters are estimated and discussion on this aspect is limited. Since the derived parameter estimates are further used for predictions at different, usually fluctuating temperature conditions, the necessity of accurately identifying those values, as well as their variability, is evident. In this context, the objective of the present work was to design a systematic kinetic approach and investigate a number of dynamic temperature profiles, of different types, in terms of their ability to generate accurate kinetic parameters with low CIs. Calculating mean values of kinetic parameters is not adequate; asymptotic CIs and joint confidence regions of the estimated parameters are of equal importance, in order to assess time-varying profile suitability and they will be discussed. Factors, such as the number and the location of the experimental points (i.e., the pattern and the frequency of sampling) as well as the quality of data (expressed as the percentage of error imposed on theoretical values when generating data sets to be tested) were also investigated. The goal was to provide practical suggestions, concerning time-temperature profile selection, and a methodology that could be applicable whatever temperature profiles and mathematical models are used to describe inactivation kinetics.

2 | THEORETICAL CONSIDERATIONS AND METHODOLOGY DEVELOPMENT

The mathematical/computational details pertained to published studies of kinetic parameter determination from dynamic experiments are mainly addressing three issues:

- (1) the primary and secondary kinetic models used to express the concentration versus time data and the effect of temperature on the reaction rates, respectively;
- (2) the dynamic time-temperature profiles employed;
- (3) the statistical procedure used to evaluate the kinetic parameters.

The following analysis presents a step-by-step development of the methodology employed, and without restricting its applicability, it is concentrated on thermal inactivation kinetics that could be described by the classical D - z values (Ball, 1923). In subsequent sections the present methodology is also used with different primary and/or secondary models.

According to the classical thermobacteriological approach used during thermal processing of foods (Ball, 1923; Bigelow, 1920) inactivation is described by Equation (1):

$$\log\left(\frac{C}{C_0}\right) = -\frac{t}{D_T} \quad (1)$$

where D_T , the decimal reduction time, is defined as the time in minutes, at constant temperature, required to reduce the initial concentration of a thermolabile substance by 90%; C , the concentration at time t ; and C_0 , the initial concentration of the thermolabile substance.

Based on Equation (1) and the application of linear regression, the D_T value is determined at each temperature of the isothermal experiments from the negative reciprocal of the corresponding slope. The temperature dependence of D_T is characterized by the z -value, that is, the increase in temperature necessary to induce a 10-fold reduction in D_T (Equation 2):

$$\log D_T = \log D_{T_{ref}} + \frac{T_{ref} - T}{z} \quad (2)$$

where T_{ref} is a reference temperature. Parameter z is determined as the negative reciprocal of the slope of $\log D_T$ vs. T regression line.

Alternatively, a global one-step approach can be applied, in which the model parameters are determined in a single step, based on all information of the experimental dataset as a whole and performing a non-linear regression through Equation (3) obtained by combining Equations (1) and (2):

$$\log\left(\frac{C}{C_0}\right) = \frac{10^{\frac{T-T_{ref}}{z}} \cdot t}{D_{T_{ref}}} \quad (3)$$

When Equation (3) is used to determine the kinetic parameters $D_{T_{ref}}$ and z from experimental C/C_0 data, a constant b is introduced into the equation in order to account for

any possible error associated with C_0 values as shown in Equation (4). This parameter, b , is kept in all subsequent equations if they are treated as regression equations, that is, for parameter estimation purposes:

$$\log\left(\frac{C}{C_0}\right) = b - \frac{10^{\frac{T-T_{ref}}{z}} \cdot t}{D_{T_{ref}}} \quad (4)$$

In the case of non-isothermal experiments, which is of particular interest in this study, kinetic parameters were obtained by non-linear regression fitting of Equation (5) to the non-isothermal experimental data (Goula et al., 2018):

$$\log\left(\frac{C}{C_0}\right) = b - \frac{\int_0^t 10^{\frac{T(t)-T_{ref}}{z}} dt}{D_{T_{ref}}} \quad (5)$$

In order to assess the ability of different temperature profiles to be used for kinetic parameter estimation, simulated concentration data at different processing times were generated, for each particular profile tested, through Equation (5) and assumed b , $D_{T_{ref}}$, and z -values. Unless otherwise stated, for all temperature profiles tested, $D_{T_{ref}}$ (at a reference temperature of 120 °C) and z -values equal to 52.0 min and 31.8 °C, respectively, based on published kinetic data of L-carnitine thermal inactivation under dynamic conditions (Goula et al., 2018), along with $b = 0$, were used. Next, an intentionally low random relative error (in the range of $\pm 2.5\%$ to $\pm 5\%$) was introduced on these “theoretically calculated” concentration values, using the EXCEL function `RANDBETWEEN()`, in order to create the necessary pseudo-experimental points. Then, the assumed kinetic parameters (z , $D_{T_{ref}}$, and b) were back-calculated by non-linear regression in a MATLAB environment. In the non-linear regression, an iterative least-squares analysis was used to locate the best estimates of the kinetic parameters, minimizing the sum of squared errors until convergence, using the following equation:

$$SSE = \sum_{i=1}^n \left[\log\left(\frac{C}{C_0}\right)_{obs,i} - \log\left(\frac{C}{C_0}\right)_{pred,i} \right]^2 \quad (6)$$

Equation (6) was minimized using the Nelder–Mead simplex optimization technique (Luersen & Le Riche, 2004; Nelder & Mead, 1965). This is a direct search method that is commonly applied to find the minimum or maximum of an objective function in a multidimensional space and can provide solutions when parameters to be optimized are not *a priori* known. To obtain the optimized kinetic parameters' estimates, for each time-temperature case, the MATLAB function `fminsearch` was applied, combined with an option command, where the maximum number of iterations as well as the acceptable sensitivity error were

defined. The integral of Equation (5) was calculated using the trapezoidal integration rule of MATLAB (*trapz*), in order for any general type of time-varying temperature profile, that results in an integral that cannot be evaluated analytically, to be handled.

The estimation and the symmetry or asymmetry of the parameters' CIs is an issue of major concern for models' reliability and practical application; in the case of linear models, CIs for the parameters are exactly defined and symmetric, whereas for non-linear models, estimation of CIs is not straightforward (Goula et al., 2018). When reporting CIs for non-linear parameter estimation, it is essential to describe how these intervals were derived (Dolan et al., 2007).

For non-linear models, an established method for computing the CIs is via bootstrapping (Efron 1979; Huang & Vinyard, 2016; Joshi et al., 2006) through a Monte Carlo technique (Van Boekel, 1996) that does not depend on linear approximations. Alternatively, a common and established approximation of non-linear CIs is the calculation of the asymptotic CI, which is symmetric (Van Boekel, 1996), a procedure followed in this analysis. This approximation may underestimate the true CI (Johnson & Faunt, 1992), but, as discussed in Dolan et al. (2007), asymptotic CIs are computationally practical and conceptually attractive.

In the present work, CIs at a $(1-\alpha)$ CI were estimated as $\pm SE \cdot t_{\alpha/2, (n-p)}$ (Mishra et al., 2008; Van Boekel, 1996), using the asymptotic standard errors (SEs) and the t -distribution parameter (n being the number of observations and p the number of estimated parameters).

The SE of each parameter (SE_i) was calculated by Equation (7), SE_i being the square root of the corresponding diagonal of the symmetric "i" parameter of the variance-covariance matrix (Dolan et al., 2007). In Equation (7), J is the Jacobian matrix given by Equation (8), and the superscript T denotes the matrix/vector transpose operator. The Jacobian matrix contains the partial derivatives of the model output with respect to the model parameters evaluated at each measurement point:

$$\begin{pmatrix} SE_{D_{T_{ref}}}^2 & SE_{D_{T_{ref}},z} & SE_{D_{T_{ref}},b} \\ SE_{z,D_{T_{ref}}} & SE_z^2 & SE_{z,b} \\ SE_{b,D_{T_{ref}}} & SE_{b,z} & SE_b^2 \end{pmatrix} = (J^T \cdot J)^{-1} \cdot \frac{SSE}{n-p} \quad (7)$$

$$J = \begin{pmatrix} \frac{\partial Y_1}{\partial D_{T_{ref}}} & \frac{\partial Y_1}{\partial z} & \frac{\partial Y_1}{\partial b} \\ \cdot & \cdot & \cdot \\ \cdot & \cdot & \cdot \\ \frac{\partial Y_n}{\partial D_{T_{ref}}} & \frac{\partial Y_n}{\partial z} & \frac{\partial Y_n}{\partial b} \end{pmatrix} \quad (8)$$

where

$$Y = \log \left(\frac{C}{C_0} \right) \quad (9)$$

The MATLAB *nlparci(beta,residuals,jacobian)* function, was used to provide the 95% CI of parameters $D_{T_{ref}}$, z , and b , through calculation of the Jacobian matrix and the residuals (Equation 10):

$$\text{Residual}_i = \log \left(\frac{C}{C_0} \right)_{obs,i} - \log \left(\frac{C}{C_0} \right)_{pred,i} \quad (10)$$

It is worth noticing, however, that in our case, where the purpose is to analyze time-varying data, the covariance of the simultaneously estimated parameters cannot be neglected by solely estimating individual CIs. Thus, joint confidence regions were calculated and graphically illustrated, according to Equation (11) (Draper & Smith, 1981):

$$SSE \leq SSE(\theta) \left\{ 1 + \frac{p}{n-p} F(p, n-p, 1-\alpha) \right\} \quad (11)$$

where $SSE(\theta)$ is the least sum of squared differences, at optimal parameter values, and F is the upper $1-\alpha$ quantile for an F -distribution with p and $n-p$ degrees of freedom.

In the present work, joint confidence regions were calculated only for the two of the involved parameters, namely, the $D_{T_{ref}}$ and the z -values, for the third parameter b being kept constant during the joint confidence regions calculations at its mean estimated value.

All combinations of kinetic parameters with the sum of squared errors less than or equal to the calculated $SSE(\theta)$ values will be inside the joint confidence region. Equation (11) does not require the confidence region to have an elliptical shape (Donaldson & Schnabel, 1987; Schwaab, Biscaia, et al., 2008). The confidence regions obtained with this method (Equation 11), called likelihood confidence regions, can be disjoint and unbounded (Schwaab, Biscaia, et al., 2008). For two-parameter models, the likelihood region can be determined with standard contouring methods (Bates & Watts, 1988). All of our calculations were based on the iterative method of Motulsky and Christopoulos (2004), which can be summarized in the following procedure:

Initially, parameter 1 (along y -axis – the z -value in our case) was assigned a fixed value, equal to the best-fit value (parameter estimate) already determined. Parameter 2 (along x -axis – the $D_{T_{ref}}$ value in our case) was allowed to vary until $SSE \cong SSE(\theta)$. In general, since the contour is oval, there will be two values (roots) of parameter 2 that

will satisfy the criterion set by Equation (11). In order to complete the lower part of the contour (the part that corresponds to values of z lower than the mean), parameter 1 is assigned at a slightly lower value, $\sim 95\%$ of the best-fit value, and the previous procedure is repeated. The same steps are repeated, with constantly decreasing parameter 1 values until the two roots of parameter 2 are almost equal, such as within 1%–5% of each other. This completes the lower part of the contour. In order to complete the upper part of the contour, we repeat the previous procedure starting from parameter 1 values at 105% of the best-fit value and proceed by using increasing values. All the above mentioned repetitive process was implemented in a MATLAB environment after editing the necessary algorithm in order to identify the values of the parameter set ($D_{T_{ref}}$ and z -values) that fulfill the requirements of Equation (11).

Another area of interest is related to the importance of choosing the most appropriate reference temperature when estimating kinetic parameters. The reference temperature is usually defined as a suitable average temperature of the analyzed experimental data (Schwaab, Lemos, et al., 2008). Few studies have investigated the optimal reference temperature, which is necessary to improve the precision of parameter estimates, minimizing – in some cases as the Arrhenius equation – parameter correlation (Schwaab & Pinto, 2007). However, according to Schwaab, Lemos, et al. (2008), when the model contains more than one kinetic constant, the situation is more complicated and it becomes impossible to eliminate all the parameter correlations simultaneously. It must also be noticed that the elliptical approximation of the confidence region of parameter estimates is exact for linear models only (Schwaab & Pinto, 2007). Depending on the degree of non-linearity of the model, the confidence region can present very complex shapes (Donaldson & Schnabel, 1987). In Dolan et al. (2013), T_{ref} has been given different values while estimating the kinetic parameters. The optimum T_{ref} value was chosen at the value where the correlation coefficient between the two parameters was minimum.

In our work, after initial parameter estimation assuming a reference temperature of 120 °C, T_{ref} was allowed to vary and the corresponding joint confidence regions of the kinetic parameters ($D_{T_{ref}}$, z) were calculated and comparatively plotted; the aim was to draw some conclusions regarding T_{ref} value effect on parameter correlation. Through specific examples of different temperature profiles, it was demonstrated that the proper selection of the reference temperature in Equation (5) could lead to the estimation of uncorrelated parameters, improving significantly the precision of the parameter estimates (Schwaab & Pinto 2007). For this purpose, in the present

work, the correlation coefficient, called r , between the two main parameters $D_{T_{ref}}$ and z was evaluated using Equation (12). Its value varies between -1.0 and $+1.0$. The highest absolute value of r , $|r|$, indicates more difficulty in the estimation process (Mishra et al., 2008). As stressed out by Schwaab and Pinto (2007), as $|r|$ gets closer to 1, the parameters become more correlated and parameter estimation becomes less reliable. The high correlation between parameter estimates can be attributed to different reasons, such as inappropriate model representation, bad experimental design, and/or model non-linearities (Schwaab & Pinto, 2007):

$$r = \frac{SE_{D,z}}{SE_D \cdot SE_z} \quad (12)$$

where $SE_{D,z}$, SE_D , and SE_z are calculated from the variance–covariance matrix of Equation (7).

3 | RESULTS AND DISCUSSION

In presenting our findings, we will first dedicate a section where the correctness and the reliability of the applied procedures, that is Equations (5) to (11) and their MATLAB implementation, will be tested. In developing and suggesting commonly accepted practices and procedures for kinetic parameter determinations from dynamic temperature data, proof of proper evaluation of the integral equation (Equation 5), the determination of the mean values and their 95% CI of the kinetic parameters, and the joint CIs of the parameters are essential. Next, a number of different dynamic temperature profiles will be discussed in their ability to be used for proper kinetic parameter determinations. A separate section will be devoted to the evaluation of joint CIs of the kinetic parameters involved in order to determine their potential correlation and draw further conclusions about the appropriateness of the particular temperature profile applied.

3.1 | Validation of the procedure

The whole procedure was tested against inactivation data obtained for a linearly increasing temperature profile, a case for which analytical calculations are available (Hayakawa et al., 1969; Huang, 2013). The linear temperature profile was expressed with Equation (13), in which T_o is the initial temperature, and c (°C/min) is the linear heating rate.

$$T(t) = T_o + ct \quad (13)$$

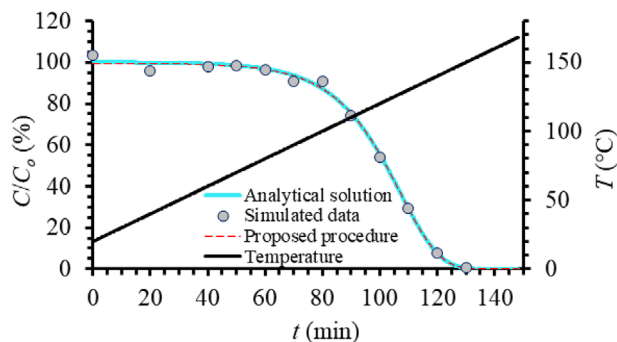


FIGURE 1 Testing of the proposed, through MATLAB, methodology (dashed black, or red when in color, line) with data from the analytical solution, Equation (14), employed through a typical, non-linear regression procedure (solid gray, or light blue when in color, line) for a linear temperature profile (solid black line). Points refer to simulating pseudo-experimental C/C_0 data

Substituting T from Equation (13) into (5), the concentration change can be calculated from Equation (14) as

$$\log\left(\frac{C}{C_0}\right) = b - \frac{\int_0^t 10^{\frac{(T_0 + ct) - T_{ref}}{z}} dt}{D_{T_{ref}}} = b - \frac{z}{\ln(10)cD_{T_{ref}}} \left[10^{\frac{(T_0 + ct) - T_{ref}}{z}} - 10^{\frac{T_0 - T_{ref}}{z}} \right] \quad (14)$$

For a linear heating temperature profile with an increasing rate of $c = 1 \text{ }^\circ\text{C}/\text{min}$, theoretical concentration versus time data were generated through Equation (14) based on the nominal $D_{120^\circ\text{C}}$ and z -values of 52.0 min and 31.8 $^\circ\text{C}$, respectively (Goula et al., 2018). On these C/C_0 values, a maximum random error up to $\pm 5\%$ was imposed in order to create simulated pseudo-experimental data. Back-estimation of the kinetic parameters was performed either with the proposed methodology based on the developed MATLAB procedure or a typical non-linear regression procedure through the analytical Equation (14) and a commercially available statistical software (SYSTAT). Kinetic parameters with the two procedures were practically identical; $D_{120^\circ\text{C}}$ values equal to 53.31 ± 1.69 min and 53.19 ± 1.60 min (mean value \pm 95% CIs) were obtained with the proposed methodology and the non-linear regression, respectively. Similarly, z -values equal to 31.10 ± 0.80 $^\circ\text{C}$ and 31.43 ± 0.79 $^\circ\text{C}$ were obtained with the proposed methodology and the non-linear regression, respectively. Thus, the validity of the proposed methodology, in comparison to analytical procedures, was established. Predicted C/C_0 values based on the kinetic parameters determined through the two procedures are depicted in Figure 1.

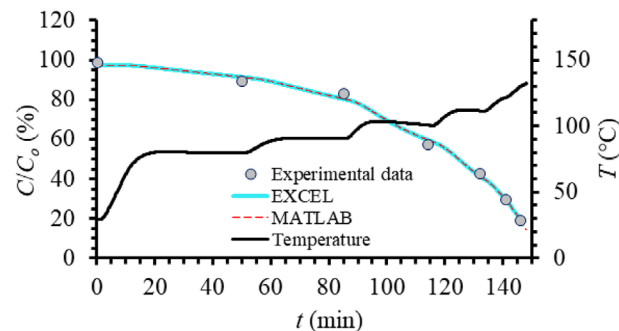


FIGURE 2 Testing of the proposed, through MATLAB, methodology (dashed black, or red when in color, line) with a semi-manual, through Microsoft EXCEL, approach (solid gray, or light blue when in color, line) for an experimental temperature profile (solid black line). Points refer to experimental literature C/C_0 data (Goula et al., 2018)

The proposed methodology, through MATLAB, was also validated using experimental C/C_0 data (Goula et al., 2018) collected during time-varying processing temperature conditions comprised of 6 temperature ramp segments, each ramp following a constant temperature period (Figure 2), and against the procedure proposed by Goula et al. (2018). Goula et al. (2018) used the same equations like the ones presented here but in a semi-manual approach through Microsoft EXCEL. Note that for this case, there is no analytical solution for the integral appearing in Equation (5). Again, practically identical $D_{120^\circ\text{C}}$ and z -values, equal to 51.9 ± 9.9 min and 31.8 ± 6.5 $^\circ\text{C}$, respectively, through MATLAB, compared to 52.0 ± 9.8 min, 31.8 ± 6.0 $^\circ\text{C}$, through EXCEL, were obtained. Predicted C/C_0 values for the two procedures are depicted in Figure 2.

3.2 | Dynamic temperature profiles

After validating the methodology developed in MATLAB, the next step involved the investigation of different types of time-temperature profiles. Among an infinite number of potential dynamic profiles that could have been selected, the following profiles were chosen: experimental temperature profile used by Goula et al. (2018; Figures 3(a) and (b)), profiles involving one linearly increasing followed by one linearly decreasing segments (Figures 3(c) and (d)), sequences of linearly increasing and linearly decreasing segments (Figures 3(e) to (n)), and sequences of step-wise increasing and decreasing segments (Figures 3(o) and (p)). The logic behind the temperature profiles chosen was either to include profiles that are commonly used in the literature or to choose profiles that, according to the authors' experience, are expected to lead to either appropriate or inappropriate results. For each of

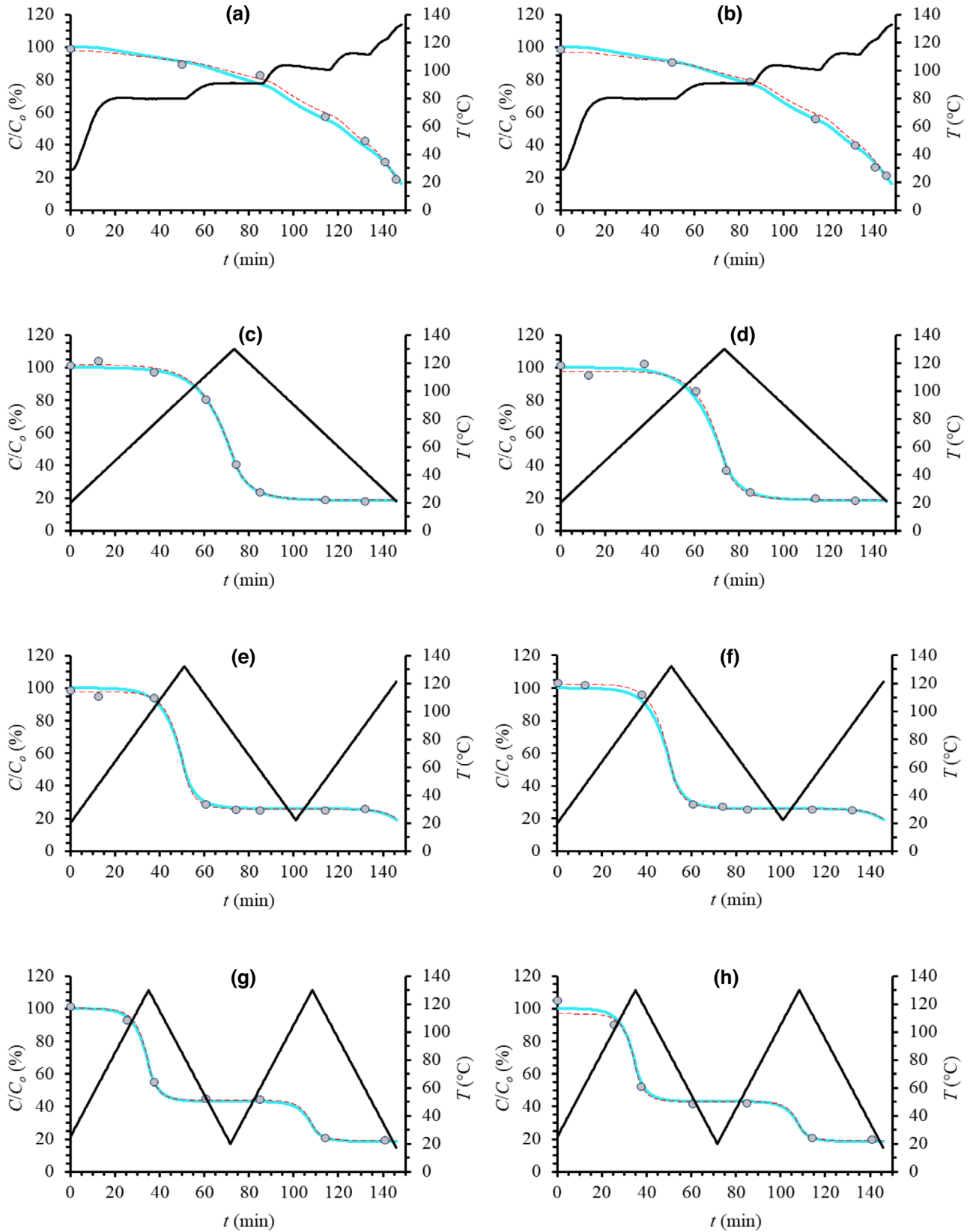


FIGURE 3 Effect of dynamic temperature profiles (solid black lines) on thermal inactivation kinetics. Solid gray, or light blue when in color, lines represent theoretical values. Points refer to simulating pseudo-experimental C/C_0 data having up to $\pm 2.5\%$ (left column) or $\pm 5.0\%$ (right column) relative error. Dashed black, or red when in color, lines are predictions based on Equation (5) and the proposed non-linear procedure. Note that an increased number of pseudo-experimental points is associated with Figures 3(k) and (l)

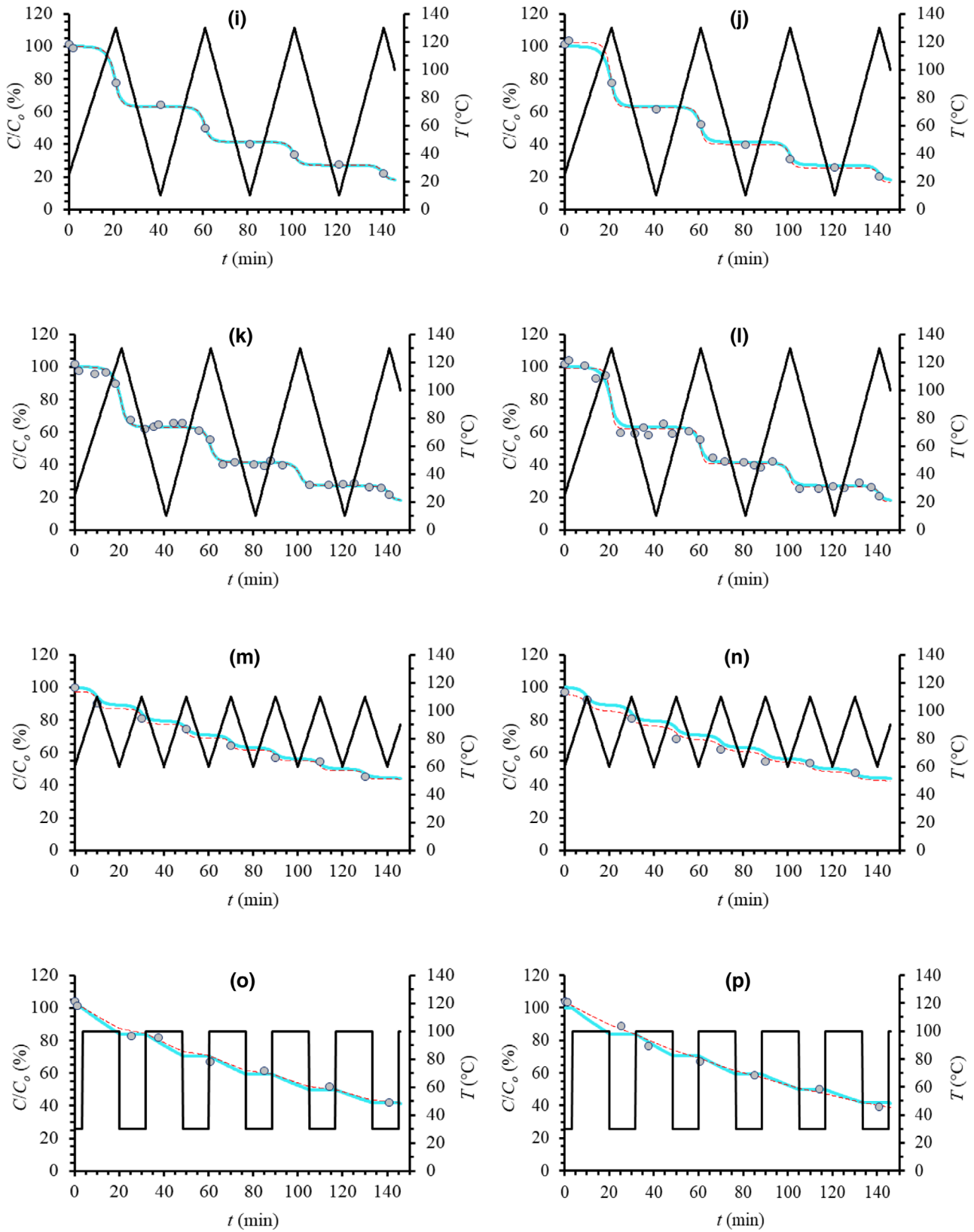


FIGURE 3 Continued

TABLE 1 Kinetic parameters, with their 95% confidence interval (CI), determined from different time-varying temperature profiles for $T_{ref} = 120\text{ }^{\circ}\text{C}$

Case	Profile type	% Error (up to \pm) ^a	Number of points	Mean	\pm 95% CI	Mean z	\pm 95% CI	Mean b	\pm 95% CI	Root mean square error (RMSE)	r
				$D_{120\text{ }^{\circ}\text{C}}$ (min)	on $D_{120\text{ }^{\circ}\text{C}}$ (min)	($^{\circ}\text{C}$)	on z ($^{\circ}\text{C}$)	on b			
1	Figure 3(a)	2.5	7	45.13	4.75	27.09	3.12	-0.0112	0.0269	0.014	0.84
2	Figure 3(b)	5	7	47.44	6.96	27.79	4.45	-0.0140	0.0321	0.018	0.25
3	Figure 3(c)	2.5	8	51.93	3.13	32.69	7.85	0.0005	0.0211	0.013	0.71
4	Figure 3(d)	5	8	51.29	3.30	26.04	10.42	-0.0101	0.0303	0.023	0.11
5	Figure 3(e)	2.5	8	52.05	2.64	25.82	7.03	-0.0122	0.0159	0.010	0.75
6	Figure 3(f)	5	8	50.54	4.89	27.99	9.04	-0.0229	0.0299	0.018	0.72
7	Figure 3(g)	2.5	7	51.48	4.19	28.28	13.56	0.0006	0.0243	0.014	0.73
8	Figure 3(h)	5	7	52.09	6.72	27.3	23.48	-0.0207	0.0297	0.024	0.90
9	Figure 3(i)	2.5	9	50.57	1259.56	27.46	4280.38	-0.0015	0.0015	0.010	1.00
10	Figure 3(j)	5	9	46.78	2802.89	20.81	11492.28	0.0102	0.0102	0.011	1.00
11	Figure 3(k)	2.5	26	52.43	5.82	32.75	12.53	-0.0004	0.0106	0.014	0.97
12	Figure 3(l)	5	26	52.53	22.18	16.16	15.63	-0.0044	0.0158	0.021	1.00
13	Figure 3(m)	2.5	8	17.91	67976.27	18.17	30600.94	-0.0122	0.0265	0.014	1.00
14	Figure 3(n)	5	8	74.93	2.89E+09	40.28	1.11E+09	-0.0188	0.0384	0.021	1.00
15	Figure 3(o)	2.5	8	205.50	858.20	157.88	1324.46	0.0064	0.0225	0.016	1.00
16	Figure 3(p)	5	8	298.11	985.99	783.24	19375.79	0.0143	0.0210	0.015	1.00

^a% of random error imposed on theoretical values to generate simulated experimental data.

the temperature profiles selected, the number of the experimental C/C_0 points used, as well as the percent relative error introduced in order to generate the simulated data, was tested. In the diagrams presented in Figure 3, the agreement between fitted and pseudo-experimental data is depicted for representative time-temperature profiles. A number of additional cases were also examined without having been included in the manuscript as they do not provide added insights. For all profiles tested, an R^2 between fitted and pseudo-experimental data of at least 0.98 was obtained.

In the diagrams presented in Figure 3, the continuous black line represents the temperature profile employed. The gray (light blue when in color) solid line depicts theoretical C/C_0 values created through Equation (5) for the given temperature profile and for $b = 0$, $D_{120\text{ }^{\circ}\text{C}} = 52.0$ min, and $z = 31.8\text{ }^{\circ}\text{C}$, while the points are simulated experimental data created from the theoretical values with the introduction of a random error up to $\pm 2.5\%$ or $\pm 5\%$. Finally, the dashed black (red when in color) line shows the predicted C/C_0 values through Equation (5) based on the kinetic parameters estimated by applying the proposed least square procedure on the simulated experimental data.

The effect of the dynamic temperature profiles used, the relative error (up to $\pm 2.5\%$ or $\pm 5\%$) introduced on the theoretical concentration values, and the number of experimental points on the determination of the $D_{120\text{ }^{\circ}\text{C}}$ and z

(and b) values, as well as their 95% CI, are presented in Table 1, along with the root mean square error (RMSE – Equation 15), a measure of the deviation of the experimental data from model predictions:

$$RMSE = \sqrt{\frac{SSE}{n - p}} \quad (15)$$

where n is the number of data points and p the number of parameters (here equals to 3).

Increasing experimental error and/or decreasing number of observations resulted in increasing uncertainty (as reflected by the $\pm 95\%$ CI) in kinetic parameters estimation. Note in some cases, the deviation of the mean kinetic parameter values from the expected ones (e.g., case 15 – Figure 3(o)) and the enormous CI are calculated (e.g., case 9 – Figure 3(i) and case 14 – Figure 3(n)) as a result of an inappropriately selected temperature profile.

From Figure 3 (graphical assessment) and Table 1 (RMSE values) one can judge the quality of fitting for each time-temperature scenario assumed. In all cases studied, both RMSE and R^2 values can be considered to describe an adequate, and frequently an excellent, fitting of the model to the experimental points. This is indicative of the appropriateness of the model and the procedure used to describe thermal inactivation under the imposed constraints. In a second step, the appropriateness of the model

for proper parameter estimation can be also judged by the mean estimates of the kinetic parameters of Equation (5) (viz., $D_{120^\circ\text{C}}$, z -value and b) and their deviation from the assumed values of 52.0, 31.8 and 0, respectively. For instance, it can be observed that in the cases of Figures 3(m), (o), (n), and (p), the mean estimates differ significantly from the assumed values. This is a direct consequence of the dynamic temperature profiles used. Going deeper in the evaluation of parameter estimation, one can also take into consideration the CIs ($\pm 95\%$ CI) of the kinetic parameters of the model and select those cases that lead to narrow CI. For example, although being classified as a good scenario based on the criterion of the value of the mean estimates, the cases of Figures 3(i) and (j) show unacceptably broad CIs for both D and z parameters.

The correlation coefficient, r , between kinetic parameters $D_{T_{ref}}$ and z -values ranged significantly for the different types of profiles tested (Table 1). According to Johnson and Frasier (1985), an $|r|$ value higher than 0.96 would be critical, whereas Bates and Watts (1988) considered 0.99 as the critical value. Dolan et al. (2007) mentioned that the correlation coefficient is highly dependent on the reference temperature. Therefore, when reporting confidence regions for parameters, it is necessary to report both the reference temperature and the correlation coefficient (Goula et al. 2018). The high $|r|$ values associated with profile types from Figures 3(i) to (p) (Table 1), could be the result of using a reference temperature of 120°C rather than an "optimum" reference temperature. The effect of the reference temperature employed on parameters correlation is discussed later in a separate section.

In order to test the underlying statistical assumptions for the kinetic parameters determination, that is, constant variance, independence of variables, normality of the distribution, as discussed in Van Boekel (1996) and Dolan and Mishra (2013), the residuals, in terms of both C/C_0 and $\log(C/C_0)$, were plotted (data not shown) and found to be centered on zero, with no particular trend, for the whole range of fitted values. Therefore, random errors imposed on theoretical values can be assumed to produce residuals that are normally distributed. Based on calculations of the residuals of the linearized equation (Equation 5), the linearized form of the model caused a larger relative error on simulated data than that imposed on the initial concentration data as has been also discussed in the literature (Van Boekel, 1996). However, the exact level of error does not disturb the validity of our methodology.

A further crucial criterion for assessing the adequacy of the profiles selected is the construction of the joint CIs (JCI). As will be discussed later in detail, from the pattern of the JCI, one can evaluate the quality of the fitting in terms of the level of correlation between the kinetic parameters studied.

3.2.1 | Commenting on the values of the kinetic parameters

In the preceding paragraphs, results and discussion were based on D and z -values equal to $D_{120^\circ\text{C}} = 52.0$ min and $z = 31.8^\circ\text{C}$, typical thermal inactivation kinetic parameters for quality indices (Lund, 1977). Nevertheless, similar conclusions can be derived when typical D and z -values for microbial thermal inactivation are used as illustrated in Figure 4 for $D_{120^\circ\text{C}} = 1$ min and $z = 10^\circ\text{C}$. For the case of a temperature profile with a single linearly increasing followed by a single linearly decreasing segments (Figure 4(a)), mean values of the kinetic parameters determined by the proposed procedure were in agreement with the theoretical values and were characterized by narrow CIs ($D_{120^\circ\text{C}} = 1.28 \pm 0.04$ min and $z = 9.93 \pm 0.38^\circ\text{C}$, Table 2). On the contrary, a temperature profile consisting of three periodical sequences, of one linearly increasing and one linearly decreasing segments (Figure 4(b)) resulted in inaccurate kinetic parameters (Table 2) as expected from the previous analysis of the data with $D_{120^\circ\text{C}} = 52.0$ min and $z = 31.8^\circ\text{C}$. In particular, due to the sampling time employed, estimations produced different shapes of inactivation curves based on the starting values of the parameters used to initiate iterations and the convergence criteria. As illustrated in Figure 4(b), the kinetic parameters in Table 2 give rise to completely different shape patterns, represented by stepwise, sinusoidal, or even straight line curves on a semi-log plot.

As it will become clear in the proceeding analysis, an integrative methodology should be applied: The appropriateness or not of a particular temperature profile to produce accurate estimates of the kinetic parameters, besides the graphical agreement and the RMSE value between experimental and estimated concentration data, the CI and the correlation coefficient of the estimated kinetic parameters, is also determined by the joint confidence regions of the parameters involved—as affected by the right choice of the reference temperature. An alternative generic scheme which, in brief, includes plotting of scaled sensitivity coefficients, performing the inverse problem, reporting parameter estimations, along with their SEs, and finally, justifying the validity of the results produced was presented by Dolan and Mishra (2013).

3.3 | Alternative primary and secondary models

The analysis presented up to now was based on the D - z approach (Equations 1 and 2) and their proper derivatives). This does not really impose a restriction on the proposed methodology. Any other appropriate primary or secondary

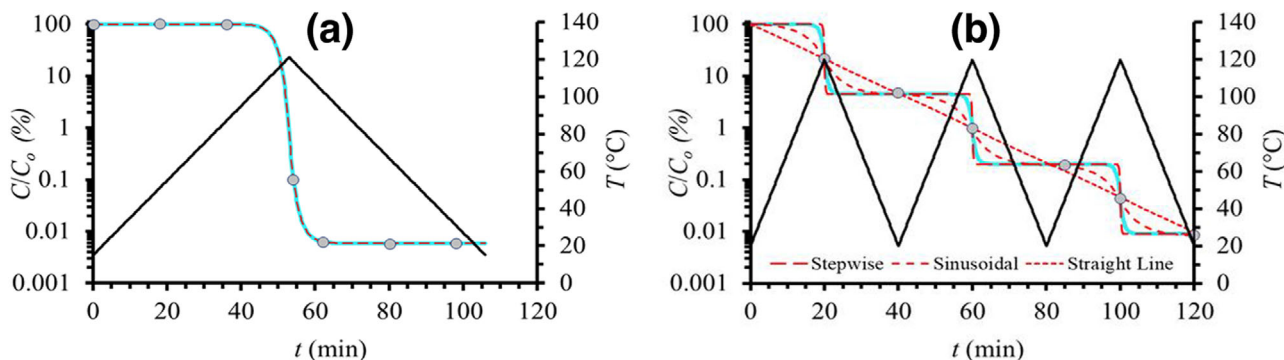


FIGURE 4 Effect of dynamic temperature profiles (solid black lines) on thermal inactivation kinetics. Solid gray, or light blue when in color, lines represent theoretical values corresponding to $D_{120^\circ\text{C}} = 1$ min and $z = 10^\circ\text{C}$. Points refer to simulating pseudo-experimental C/C_0 data having up to $\pm 5.0\%$ random relative error. Dashed black, or red when in color, lines are predictions based on Equation (5) and the proposed non-linear procedure

model, with the appropriate adjustments, could be used without altering the conclusions of this study. However, the underlying assumption in the analysis that the primary and the secondary models applied to the system under investigation were *a priori* known could be a constraint to the methodology. Indeed, one can imagine a combination of primary and secondary models that will adequately describe a set of experimental concentration versus time data obtained during time-varying conditions, with minor statistical differences in the parameters used to characterize the goodness of fit. For example, the simulated data presented in Figure 5(a) were described either by the first order (D - z) model or a Weibull-type model (Equation 16) and an appropriate secondary model (Equation 17) proposed by Chen and Campanella (2012):

$$\log S(t) = -b_1(T) \cdot t^{n_1} \quad (16)$$

where $S(t)$ is the survival ratio C/C_0 , T is a constant temperature, and b_1 and n_1 are empirical parameters. Parameter b_1 is considered as a temperature-dependent parameter, given by the following secondary model:

$$b_1(T) = \ln \{1 + \exp [k \cdot (T - T_c)]\} \quad (17)$$

where T_c and k are treated as empirical constants. Substitution of Equations (17) into (16) gives:

$$\log S(t) = -\ln \{1 + \exp [k \cdot (T - T_c)]\} \cdot t^{n_1} \quad (18)$$

Equation (18) is valid for data collected at a constant temperature. For variable temperature profiles, the differential form of Equation (16), leading to the ordinary differential equation (Equation 19), was derived (Peleg et al., 2005) assuming that the power variable n_1 is constant and that

variable $b_1(T)$ is given by Equation (17):

$$\frac{d(\log S(t))}{dt} = -b_1 [T(t)] n_1 \left(\frac{-\log S(t)}{b_1 [T(t)]} \right)^{(n_1-1)/n_1} \quad (19)$$

Thus, for variable temperature profiles, an iterative method, such as the one developed by Peleg et al. (2005) and also applied by Chen et al. (2007) should be used to analyze inactivation data. The implementation of this method (Peleg et al., 2005), called the “incremental” version, is based on the discretization of the dynamic profile to small-time intervals, where the temperature is assumed to remain constant and estimated by the average temperature during that time period. Using this iterative method, the parameters k , T_c , and n_1 were determined for the simulated data and the temperature profile of Figure 3(b) (Table 1, case 2). The comparison between the predicted and the simulated data is presented in Figure 5(a). As can be seen, the Weibull-type model together with the secondary model just described, that is, Equation (19), gave appropriate predictions (Figure 5(a) and Table 3). For the same data, the first order D - z model has been employed with satisfactory results (Figure 3(b) and Table 1) and for comparison purposes are plotted again on Figure 5(a). As can be seen from Figure 5(a) and Tables 1 and 3, both kinetic models (using first-order or Weibull as the primary model) adequately described the experimental data, and there was no apparent reason to select the one over the other. However, in reference to Figure 5, the use of the kinetic parameters determined from data for the temperature profile of Figure 5(a) to a different temperature profile, that is, the temperature profile of Figure 5(b) gave predictions of survival ratios clearly distinguishable for the two models. From preliminary data (not shown) this is mainly an effect of the differences in the primary rather than the secondary

TABLE 2 Kinetic parameters, with their 95% CI, determined from the data presented on Figure 4

Case	Profile type	Mean $D_{120^\circ\text{C}}$ (min)	$\pm 95\%$ CI on $D_{120^\circ\text{C}}$ (min)	Mean z ($^\circ\text{C}$)	$\pm 95\%$ CI on z ($^\circ\text{C}$)	Mean b	$\pm 95\%$ CI on b	RMSE	$ r $	Optimum T_{ref} ($^\circ\text{C}$)	Mean $D_{T_{ref}}$ (min)	$\pm 95\%$ CI on $D_{T_{ref}}$ (min)	Calculated $D_{120^\circ\text{C}}$ (min) ^a	$\pm 95\%$ CI on Calculated $D_{120^\circ\text{C}}$ (min)
1	Figure 4(a)	1.28	0.04	9.93	0.38	-0.0084	0.0130	0.0081	0.993	117.0	2.58	0.01	1.29	0.004
2	Figure 4(b) (stepwise)	1.42	3.19E+09	13.21	2.51E+07	-0.0186	0.0074	0.0191						
3	Figure 4(b) (sinusoidal)	7.24	6.52	57.73	55.94	0.0222	0.0045	0.0151	0.999	96.5	18.50	0.37	7.24	0.140
4	Figure 4(b) (line)	28.26	47.44	2036.60	6.39E+04	0.0000	-	0.0269						

^aBased on Equation (2).

models employed. Thus, for systems where the primary and the secondary kinetic models are not known, it is suggested to use additional data for a second time-varying temperature profile in order for the appropriate kinetic models to be selected (Cattani et al., 2016; Huang, 2020; Huang & Li, 2020).

3.4 | Joint confidence regions–correlation of the parameters

The individual 95% CIs on the kinetic parameters presented and discussed so far indicated the confidence by which each of the parameters was determined. However, in order to make conclusions about the ability of the temperature profiles investigated to generate uncorrelated parameters, the joint confidence regions between the parameters involved had to be determined.

The shape and the particular form of the joint confidence region *per se* provide useful information on the reliability, uncertainty, and correlation of the parameter estimates. A joint confidence region of parameter estimates can be defined as a hyper-ellipsoid in the parameter space. When parameters are not correlated, the axes of the hyper-ellipsoid are parallel to the parameter axes. It must be noticed that the elliptical approximation of the confidence region of parameter estimates is exact only for linear models. Regarding the shape of the curves in the case of non-linear models (such as the ones used in this work), the contours are often asymmetric about the estimate and may be twisted, with the shape of p-dimensional bananas (Atkinson & Donev, 1992). The higher the correlation, the more stretched ellipse (deviation from a cycle) will be the shape of the joint confidence region (Dolan et al., 2007). Depending on the degree of non-linearity of the model, the confidence region can present very complex shapes (Donaldson & Schnabel, 1987; Schwaab & Pinto, 2007). Schwaab, Biscaia, et al. (2008) studied the confidence regions of kinetic constants in non-linear models and concluded that the confidence regions can be non-convex, open, and constituted by disconnected regions.

The joint confidence regions of the main parameters, $D_{T_{ref}}$ and z -values (keeping the b value fixed at its mean estimate) were calculated (through Equation 11) for data from a number of representative time-varying temperature profiles and depicted in Figure 6 for some particular cases. The selected cases refer to profiles from Table 1 representative of good or bad examples in estimating the mean values and/or the $\pm 95\%$ CIs of the kinetic parameters. In the corresponding figures (Figure 6), x -axis depicts the $D_{T_{ref}}$ value and y -axis the z -value. For all cases, plots were calculated assuming a reference temperature of 120 $^\circ\text{C}$. The effect of T_{ref} choice on the joint confidence regions and

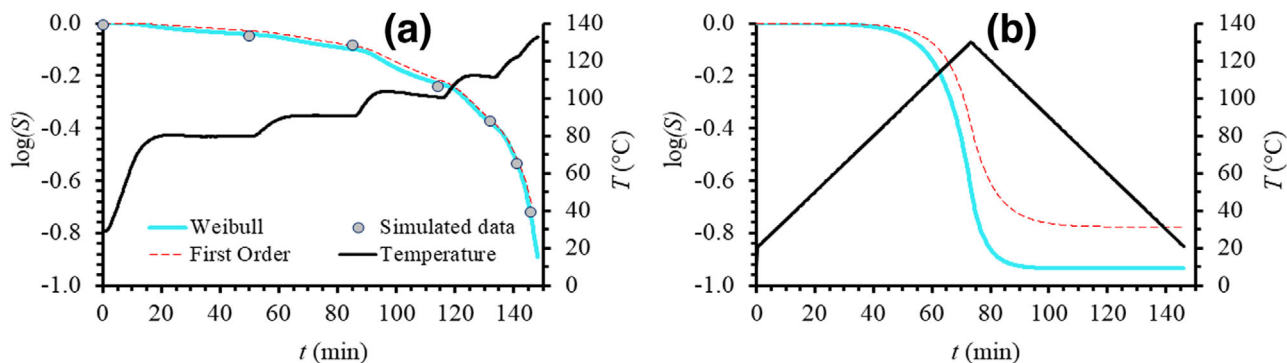


FIGURE 5 Effect of different models on thermal inactivation kinetics for particular dynamic temperature profiles (solid black lines). Points on Figure 5(a) refer to simulating pseudo-experimental C/C_0 data obtained with the proposed D - z model with up to $\pm 5.0\%$ added relative error. Solid gray, or light blue when in color, lines represent predictions using Equation (19) (Weibull), while dashed black, or red when in color, lines are predictions using the D - z model (first-order)

TABLE 3 Kinetic parameters, with their 95% CI, determined using Equation (19), associated with a Weibull type model as primary model, and the time-varying temperature profile of Figure 5(a)

Primary model used	Profile type	Number of points	Mean k ($^{\circ}\text{C}^{-1}$)	\pm 95% CI on k ($^{\circ}\text{C}^{-1}$)	Mean T_c ($^{\circ}\text{C}$)	\pm 95% CI on T_c ($^{\circ}\text{C}$)	Mean n_1	\pm 95% CI on n_1	RMSE
Equation (4)	Figure 5(a)	7	0.0745	0.00876	149.25	24.584	0.583	0.301	0.00491

correlation of the parameters will be discussed in the next section.

The joint CIs at a confidence level of 90%, 95%, and 99% are depicted in Figure 6(a) for the data associated with the temperature profile of Figure 3(a). Note that according to Haralampu et al. (1985), the extremes of the 90% joint confidence ellipses correspond approximately to the ends of the 95% individual CIs of the parameter estimates (the joint probability of two events at 95% probability is approximately 90%, i.e., $0.95^2 \approx 0.90$). Joint confidence regions, depicted in Figure 6(a), have a normal, ellipsoid shape, and although the axes of the ellipses are not parallel to the coordinate axes, they imply that the use of a profile, such as the one depicted in Figure 3(a), leads to the accurate prediction of parameters, with small 95% CI, and acceptable JCI.

As presented in Table 1, profiles of Figures 3(c) and (d) have an acceptable performance, based both on the parameter estimates' closeness to the assumed values as well as the small 95% CI. Their JCI, as depicted in Figures 6(b) and (c), although deviating from an ideal ellipsoid, can be considered as acceptable, regarding parameter correlation. The higher error introduced in Figure 3(d) C/C_0 data, compared to Figure 3(c), is considered responsible for the tailing effect observed for the larger $D_{120^{\circ}\text{C}}$ (greater than 55 min) and the lower z (lower than 15°C) values.

Data for temperature profiles like the ones shown in Figure 3(j) (acceptable estimates but large 95% CI) or Figures 3(n) and (o) (where both criteria—estimates and 95% CI—are not met) provided shapes of joint confidence

regions confirming and emphasizing the weakness of using them to predict kinetic parameters. Figure 6(d) presents an example of an open, unbounded, structure of JCI for the case of Figure 3(j) data, while Figures 6(e) and (f) depict similar behavior of joint confidence regions for data from Figures 3(n) and (o), respectively. These confidence regions deviate significantly from the ellipsoid and the confidence region grows continuously in one direction as the corresponding parameter increases (Enswailer et al., 2014; Schwaab, Biscaia, et al., 2008). In reference to Figure 6(e), unrealistic $D_{120^{\circ}\text{C}}$ values of, for example, 350 min, associated with unrealistic also and a practically infinite number of z -values ($z > 400^{\circ}\text{C}$) can give acceptable predictions. One should also notice the symmetrical disconnected joint confidence regions presented in Figure 6(f) for the data in Figure 3(o) (also observed for the data in Figure 3(n) although we did not show it in Figure 6(e)).

As anticipated, the increased number of experimental points used with the same temperature profile, that is, 26 versus 9 points for the Figures 3(l) versus (j) cases, respectively, can lead to a more acceptable JCI (Figure 6(g)). In relation to Figure 6(g), an interesting pattern can be observed; for some specific values of $D_{T_{ref}}$, there are two distinct intervals where z parameter values are inside the confidence region. According to Ensweiler et al. (2014), this behavior could be attributed to the possible dependence among estimated parameter values, although very narrow ellipses are expected for confidence regions of highly correlated parameters.

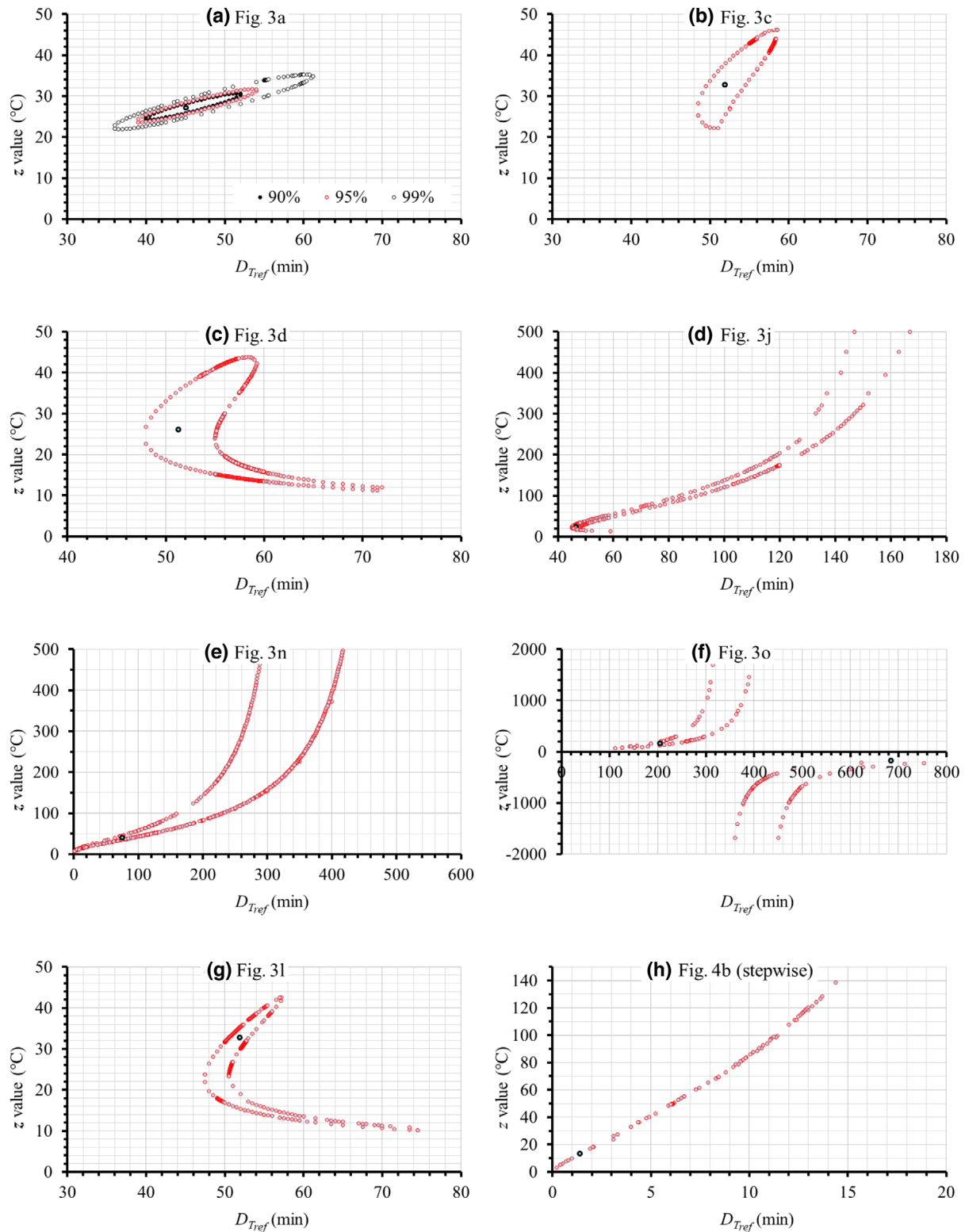



FIGURE 6 95% (unless otherwise explicitly stated) joint confidence regions from $D_{T_{ref}}$ - z estimates for indicative time-varying profiles for T_{ref} equal to 120 °C. Figure 6(a) refers to Figure 3(a) data, Figure 6(b) to Figure 3(c) data, and so on, as indicated on the top of each graph. Bold, black-bordered points, , refer to the estimated mean values of the parameters

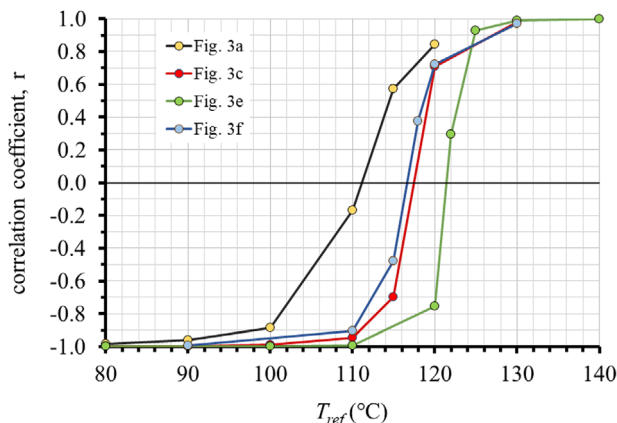


FIGURE 7 Graphical selection of the optimum reference temperature (where r equals to zero) for selected temperature profiles

It must be also observed that, in most cases, confidence regions are not symmetric with respect to the optimum estimated parameter values, indicating that the parameter deviations depend on the actual parameter values (Enzweiler et al., 2014). For example, in Figure 6(b) (for the data from Figure 3(c)), for the estimate of $D_{120^\circ\text{C}}$, equal to 51.9 min, its lower bound is around 48.5 min and the upper bound is slightly higher than 58.5 min. The same stands also for other profiles (e.g., Figures 6(a) and (c)).

Finally, for the data of Figure 4(b) (stepwise), the joint confidence region forms a very narrow and slightly curved surface, an almost line-approaching shape (Figure 6(h)) indicating that the parameter estimates are highly correlated (Schwaab & Pinto, 2007), that is, to any arbitrary value of one of the parameters corresponds a fixed value of the other parameter as indicated from the joint correlation “line”. For example, a $D_{120^\circ\text{C}}$ - z pair of 11.1 min and 97.2°C (Figure 6(h)) gives equally acceptable predictions with those obtained with the mean $D_{120^\circ\text{C}}$ - z estimates of 1.42 min and 13.21°C (Table 2, case 2). At this point, it is worth stressing out that due to the existence of high correlations among model parameters, numerical procedures used for minimization of objective functions (in our case Equation 11) could be unable to locate the JCI. In this case, a point-by-point iterative procedure for the location of every point of the JCI, as described in the *Theoretical Considerations and Methodology Development* section, was employed.

3.5 | Effect of the reference temperature, T_{ref}

The role of the reference temperature, T_{ref} , in affecting parameter correlation has been recently given attention.

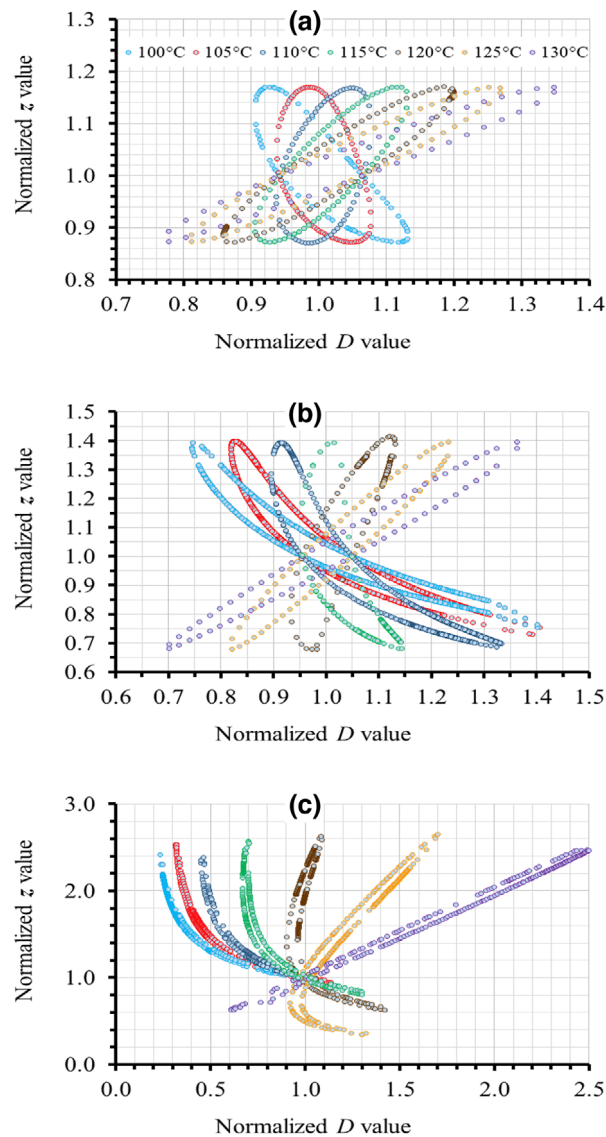


FIGURE 8 Effect of T_{ref} on parameter correlation as depicted from the joint confidence regions of the normalized D - z parameters. Figure 8(a) refers to Figure 3(a) data, Figure 8(b) refers to Figure 3(c) data and Figure 8(c) refers to Figure 3(l) data. Reading the diagrams on the top of each figure from the left to the right, T_{ref} values of 100, 105, 110, 115, 120, 125, and 130°C were used

Through reparameterization of the Arrhenius equation, Schwaab and Pinto (2007) and Schwaab, Lemos, et al. (2008) showed, both analytically and numerically, that the proper selection of the reference temperature can reduce or even eliminate the parameter correlation in kinetic models, improving—at the same time—the precision of the parameter estimates. In another work of the same group, the same methodology was followed for the reduction of parameter correlations in power-law models (Schwaab & Pinto, 2008).

To alleviate possible concerns that the selection of an optimum temperature profile could be a function of the

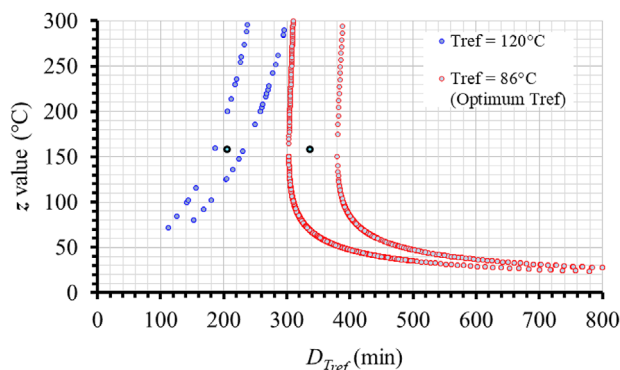
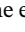


FIGURE 9 Effect of T_{ref} choice on the joint confidence regions of the $D_{T_{ref}}$ - z parameters for Fig. 3o temperature profile. Bold, black-bordered points, , refer to the estimated mean values of the parameters

reference temperature used in performing the relevant calculations, for the temperature profiles depicted in Table 1, we estimated the optimum reference temperature as the one giving rise to $|r|$ values close to zero (Figure 7) and recalculated the kinetic parameters (Table 4). For comparison purposes, $D_{T_{ref}}$ values and their 95% CI were converted to the corresponding $D_{120^\circ\text{C}}$ estimates through Equation (2). Note that as the correlation coefficient criterion (Equation 12), regarding the calculation of the optimum reference temperature, is equivalent and provided the same results with the application of the D-optimality condition of maximizing the determinant of $(J^T \cdot J)$; Equations 7 and 8) the corresponding calculations were not included within the text.

As can be seen, by comparing Table 1 with $D_{120^\circ\text{C}}$ values of Table 4, mean values remained unchanged while the corresponding 95% CIs were reduced, as expected, the reduction being noticeable for profiles where optimum T_{ref}

deviated from 120°C (case 15, Figure 3(o)). Nevertheless, z -values and their 95% CIs remained unchanged (Dolan et al., 2013; Schwaab & Pinto, 2007), high or low depending on the applicability of the particular dynamic temperature profile for kinetic parameter determination, as has been discussed in the preceding sections. Similar results are shown for cases 1 and 3 of Table 2.

In order to observe the effect of the reference temperature on the parameter correlation, as depicted by the corresponding joint confidence regions, the reference temperature was allowed to vary, as shown in Figure 8, where the normalized D and z -values are plotted (Goula et al., 2018). Although all initial calculations were performed assuming a reference temperature of 120°C , in a next step, the T_{ref} was allowed to assume different values and the covariance matrix of parameter estimates was recalculated each time, deriving the corresponding parameter correlation and the relative errors of parameter estimates (Goula et al., 2018). The mean D and z -values obtained for each T_{ref} were used to calculate the normalized D and z -values.

Figure 8 shows that in some cases of the alternative temperature profiles analyzed, uncorrelated model parameters can be obtained for a particular T_{ref} leading to better parameter estimations (Schwaab, Biscaia, et al., 2008). Figure 8 allows for the graphical approximation of the optimum reference temperature for representative temperature profiles of Figure 3. In reference to Figure 8(a) (for the data from Figure 3(a)) when the optimum reference temperature is used (close to 112°C , Table 4), the parameter confidence region becomes almost circular, indicating that uncorrelated parameters can be estimated (Schwaab & Pinto, 2008). For the data from Figure 3(c) (Figure 8(b)), the optimum reference temperature is very close to 120°C , approximately 118°C (Table 4). When moving away from the optimum

TABLE 4 Effect of T_{ref} on the kinetic parameters determined for Figure 3(m) data

Case	T_{ref} ($^\circ\text{C}$)	Mean			Mean z ($^\circ\text{C}$)	$\pm 95\%$ CI on z ($^\circ\text{C}$)	Mean b	$\pm 95\%$ CI on b	RMSE	$ r $	Calculated $D_{120^\circ\text{C}}$ (min) ^a
		$D_{T_{ref}}$ (min)	$\pm 95\%$ CI on $D_{T_{ref}}$ (min)	$\pm 95\%$ CI on $D_{T_{ref}}$ (min)							
1	60	624.11	$1.03\text{E} + 05$	140.55	$5.00\text{E} + 04$	-0.0121	0.02654	0.0135	0.999	233.54	
2	70	511.96	$5.17\text{E} + 04$	158.85	$6.15\text{E} + 04$	-0.0121	0.02654	0.0135	0.999	248.01	
3	80	578.41	$7.61\text{E} + 04$	57.63	$1.48\text{E} + 04$	-0.0122	0.0263	0.0135	0.999	116.99	
4	90	425.89	$4.88\text{E} + 04$	37.97	$1.18\text{E} + 04$	-0.0122	0.0265	0.0135	0.999	69.06	
5	105	110.77	$9.88\text{E} + 05$	10.24	$6.78\text{E} + 05$	-0.0122	0.0202	0.0135	0.999	3.80	
6	110	22.48	$4.51\text{E} + 08$	6.37	$1.31\text{E} + 08$	-0.0122	0.0258	0.0135	0.999	0.61	
7	120	17.91	$6.80\text{E} + 04$	18.17	$3.06\text{E} + 04$	-0.0120	0.0264	0.0135	0.999	17.91	
8	130	15.12	$2.31\text{E} + 04$	25.88	$1.45\text{E} + 04$	-0.0122	0.0265	0.0135	0.999	36.81	
9	135	18.06	$1.85\text{E} + 04$	32.01	$1.21\text{E} + 04$	-0.0122	0.0265	0.0135	0.999	53.12	
10	140	14.04	$1.51\text{E} + 04$	33.18	$1.20\text{E} + 04$	-0.0122	0.0265	0.0135	0.999	56.25	

^aBased on Equation (2).

TABLE 5 Optimum reference temperatures and corresponding kinetic parameters for different time-varying temperature profiles

Case	Profile type	Optimum T_{ref} (°C)	Mean $D_{T_{ref}}$ (min)	\pm 95% CI on $D_{T_{ref}}$ (min)	Mean z (°C)	\pm 95% CI on z (°C)	Calculated $D_{120^\circ C}$ (min) ^a	\pm 95% CI on Calculated $D_{120^\circ C}$ (min)	r
1	Figure 3(a)	112	89.08	4.40	27.09	3.12	45.13	2.23	0.18
2	Figure 3(b)	111	100.00	7.73	27.79	4.45	47.44	3.66	0.07
3	Figure 3(c)	118	59.79	2.61	32.69	7.85	51.93	2.27	0.20
4	Figure 3(d)	120	51.29	3.30	26.04	10.42	51.29	3.30	0.11
5	Figure 3(e)	122	43.54	1.53	25.82	7.03	52.05	1.82	0.29
6	Figure 3(f)	117	63.77	4.59	27.99	9.04	49.83	3.59	0.01
7	Figure 3(g)	118	60.59	3.55	28.28	13.56	51.48	3.02	0.32
8	Figure 3(h)	122	42.26	3.05	27.30	23.48	50.02	3.62	0.20
9	Figure 3(i)	a	—	—	—	—	—	—	—
10	Figure 3(j)	a	—	—	—	—	—	—	—
11	Figure 3(k)	116	69.45	1.92	32.75	12.53	52.43	1.45	0.00
12	Figure 3(l)	123	34.25	1.40	16.16	15.63	52.53	2.15	0.16
13	Figure 3(m)	a	—	—	—	—	—	—	—
14	Figure 3(n)	a	—	—	—	—	—	—	—
15	Figure 3(o)	86	337.42	37.88	157.88	1324.46	205.50	23.07	0.13
16	Figure 3(p)	a	—	—	—	—	—	—	—

Note: ^a: not found through the algorithm implemented.

^aBased on Equation (2).

T_{ref} , joint confidence regions become more elliptical and slanted either to the left or to the right. Finally, for the data from Figure 3(l) (Figure 8(c)), the optimum reference temperature (approximately 123 °C, Table 4) provides a more appropriate joint confidence region, minimizing the two distinct intervals where z parameter values were located for specific values of $D_{T_{ref}}$ observed for other reference temperatures including the T_{ref} of 120 °C (Figure 6(g)).

In relation to the main objective of the present work, the kinetic parameters and the appropriate statistics were calculated for different T_{ref} values for a number of temperature profiles that up to now were evaluated as improper. In particular, for the data in Figure 3(m), the estimated $D_{T_{ref}}$, z , and b values together with associated (calculated) $D_{120^\circ C}$ are presented in Table 4. As can be inferred from Table 4, based on the high 95% CI and the deviation of the $D_{120^\circ C}$ and z -values from the originally used ones to generate the pseudo-experimental C/C_0 data (of 52.0 min and 31.8 °C, respectively), the choice of the reference temperature does not improve the performance of the particular profiles. This is proven, for $T_{ref} = 120$ °C, by the corresponding value of the correlation coefficient, that is, close to 1 (Table 1). The same holds for the other reference temperatures tested, where there was a weakness to select the optimum reference temperature. This was also noticed for temperature profiles in Figures 3(i), (j), (n)), and 3(p) (Table 5).

As far as joint CIs are concerned, the employment of an optimum reference temperature does not necessarily affect conclusions arising through joint confidence regions observations. As shown in Figure 9, for Figure 3(o) temperature profile, the choice of T_{ref} , although it alters the shape of the joint confidence regions, does not render that particular profile acceptable for both $D_{T_{ref}}$ - z parameter estimations.

4 | CONCLUSION

Determination of inactivation kinetics from concentration versus time data obtained under dynamic temperature conditions, involves more complicated and elaborated data analysis and interpretation but requires less experimental effort, compared to isothermal data analysis. Thermal inactivation kinetics, described by the classical D - z values, were initially used as a case study to demonstrate the use of the proposed methodology in order to determine inactivation kinetic parameters from experimental time-varying temperature conditions of any form. The selection of a particular dynamic temperature profile is crucial and greatly affects the feasibility of such a procedure. From all different time-varying profiles tested, those giving rise to concentration versus heating time curves deviating from typical first-order kinetic lines were found to provide more accurate, and with a rather small CIs, estimations

of the kinetic parameters. Estimation of the joint CIs also revealed cases that lead to parameters highly correlated, not allowing for reliable parameter estimations. The selection of an appropriate reference temperature does influence joint CIs, without altering the ability of a particular temperature profile to be used for parameter estimation. In reference to the profiles tested, stepwise increasing or single triangle-shaped temperature profiles are the recommended profiles for proper kinetic parameter evaluation. As shown, the same procedure can be employed when a different primary or secondary model is used to describe kinetic data. When the primary model mainly, and to a lesser extent the secondary model, is not *a priori* known, data collection for at least two different time-varying temperature profiles is suggested.

AUTHOR CONTRIBUTIONS

Maria Giannakourou: Data curation-Equal; Formal analysis-Equal; Investigation-Equal; Methodology-Equal; Software-Equal; Validation-Equal; Visualization-Equal; Writing-original draft-Equal; Writing-review & editing-Equal. Konstantinos-Philip Saltaouras: Data curation-Equal; Formal analysis-Equal; Investigation-Equal; Methodology-Equal; Software-Equal; Validation-Equal. N Stoforos: Conceptualization-Lead; Data curation-Equal; Formal analysis-Equal; Investigation-Equal; Methodology-Equal; Project administration-Lead; Resources-Lead; Software-Equal; Supervision-Lead; Validation-Equal; Visualization-Equal; Writing-original draft-Equal; Writing-review & editing-Equal.

CONFLICT OF INTEREST

The authors declare that there are no conflicts of interest.

ORCID

Maria C. Giannakourou  <https://orcid.org/0000-0002-3625-2950>

Nikolaos G. Stoforos  <https://orcid.org/0000-0002-9737-9568>

REFERENCES

- Aghajanzadeh, S., Ziaififar, A. M., Kashaninejad, M., Maghsoudlou, Y., & Esmailzadeh, E. (2016). Thermal inactivation kinetic of pectin methylesterase and cloud stability in sour orange juice. *Journal of Food Engineering*, *185*, 72–77. <https://doi.org/10.1016/j.jfoodeng.2016.04.004>
- Aragao, G. M. F., Corradini, M. G., Normand, M. D., & Peleg, M. (2007). Evaluation of the Weibull and log normal distribution functions as survival models of *Escherichia coli* under isothermal and non isothermal conditions. *International Journal of Food Microbiology* *119*(3), 243–257. <https://doi.org/10.1016/j.ijfoodmicro.2007.08.004>
- Atkinson, A. C., & Donev, N. (1992). *Optimum experimental designs*. Oxford University Press.
- Ball, C. O. (1923). *Bulletin of the National Research Council No. 37* (Vol 7, Part 1). National Research Council.
- Bates, D. M., & Watts, D. G. (1988). *Nonlinear regression analysis and its applications*. John Wiley & Sons, Inc
- Bernaerts, K., Versyck, K. J., & Van Impe, J. F. (2000). On the design of optimal dynamic experiments for parameter estimation of a Ratkowsky-type growth kinetics at suboptimal temperatures. *International Journal of Food Microbiology*, *54*(1–2), 27–38. [http://doi.org/10.1016/S0168-1605\(99\)00140-3](http://doi.org/10.1016/S0168-1605(99)00140-3)
- Bernaerts, K., Servaes, R. D., Kooyman, S., Versyck, K. J., & Van Impe, J. F. (2002). Optimal temperature input design for estimation of the square root model parameters: parameter accuracy and model validity restrictions. *International Journal of Food Microbiology*, *73*(2–3), 145–157. [http://doi.org/10.1016/S0168-1605\(01\)00645-6](http://doi.org/10.1016/S0168-1605(01)00645-6)
- Bigelow, W. D., Bohart, G. S., Richardson, A. C., & Ball, C. O. (1920). *Heat penetration in processing canned foods.*, *Bulletin 16-L*, Research Laboratory, National Canners Association.
- Cao, X., Cai, C., Wang, Y., & Zheng, X. (2018). The inactivation kinetics of polyphenol oxidase and peroxidase in bayberry juice during thermal and ultrasound treatments. *Innovative Food Science & Emerging Technologies* *45*, 169–178. <https://doi.org/10.1016/j.ifset.2017.09.018>
- Cattani, F., Dolan, K. D., Oliveira, S. D., Mishra, D. K., Ferreira, C. A. S., Periago, P. M., Aznar, A., Fernandez, P. S., & Valdramidis, V. P. (2016). One-step global parameter estimation of kinetic inactivation parameters for *Bacillus sporothermodurans* spores under static and dynamic thermal processes. *Food Research International*, *89*, 614–619. <https://doi.org/10.1016/j.foodres.2016.08.027>
- Chen, G., Campanella, O. H., & Corvalan, C. M. (2007). A numerical algorithm for calculating microbial survival curves during thermal processing. *Food Research International*, *40*, 203–208. <https://doi.org/10.1016/j.foodres.2006.09.009>
- Chen, G., & Campanella, O. H. (2012). An optimization algorithm for estimation of microbial survival parameters during thermal processing. *International Journal of Food Microbiology*, *154*(1), 52–58. <https://doi.org/10.1016/j.ijfoodmicro.2011.12.019>
- Cheng, X. -f., Zhang, M., & Adhikari, B. (2013). The inactivation kinetics of polyphenol oxidase in mushroom (*Agaricus bisporus*) during thermal and thermosonic treatments. *Ultrasonics Sonochemistry*, *20*(2), 674–679. <https://doi.org/10.1016/j.ultsonch.2012.09.012>
- Claeys, W. L., Ludikhuyze, L. R., Van Loey, A. M., & Hendrickx, M. E. (2001). Inactivation kinetics of alkaline phosphatase and lactoperoxidase, and denaturation kinetics of β -lactoglobulin in raw milk under isothermal and dynamic temperature conditions. *Journal of Dairy Research*, *68*(1), 95–107. <https://doi.org/10.1017/S002202990000460X>
- Conesa, R., Periago, P. M., Esnoz, A., López, A., & Palop, A. (2003). Prediction of *Bacillus subtilis* spore survival after a combined non-isothermal-isothermal heat treatment. *European Food Research and Technology*, *217*(4), 319–324. <https://doi.org/10.1007/s00217-003-0749-5>
- Cornet, I., Van Derlinden, E., Cappuyns A. M., & Van Impe, J. M. (2010). Heat stress adaptation of *Escherichia coli* under dynamic conditions: effect of inoculum size. *Letters in Applied Microbiology*, *51*, 450–455. <https://doi.org/10.1111/j.1472-765X.2010.02920.x>
- Corradini, M. G., Normand, M. D., & Peleg, M. (2005). Calculating the efficacy of heat sterilization processes. *Journal of Food Engineering*, *67*(1–2), 59–69. <https://doi.org/10.1016/j.jfoodeng.2004.08.001>

- Corradini, M. G., Normand, M. D., & Peleg, M. (2006). Expressing the equivalence of non-isothermal and isothermal heat sterilization processes. *Journal of the Science of Food and Agriculture*, 86(5), 785–792. <https://doi.org/10.1002/jfsa.2416>
- Corradini, M. G., & Peleg, M. (2007). A Weibullian model for microbial injury and mortality. *International Journal of Food Microbiology*, 119(3), 319–328. <https://doi.org/10.1016/j.ijfoodmicro.2007.08.035>
- Corradini, M. G., Normand, M. D., & Peleg, M. (2008). Prediction of an organism's inactivation patterns from three single survival ratios determined at the end of three non-isothermal heat treatments. *International Journal of Food Microbiology*, 126(1), 98–111. <https://doi.org/10.1016/j.ijfoodmicro.2008.05.007>
- Cunha, L. M., & Oliveira F. A. R. (2000). Optimal experimental design for estimating the kinetic parameters of processes described by the first-order Arrhenius model under linearly increasing temperature profiles. *Journal of Food Engineering*, 46, 53–60. [https://doi.org/10.1016/S0308-8146\(00\)00138-2](https://doi.org/10.1016/S0308-8146(00)00138-2)
- Dolan, K. D. (2003). Estimation of kinetic parameters for non-isothermal food processes. *Journal of Food Science*, 68(3), 728–741. <https://doi.org/10.1111/j.1365-2621.2003.tb08234.x>
- Dolan, K. D., Yang, L., & Trampel, C. P. (2007). Nonlinear regression technique to estimate kinetic parameters and confidence intervals in unsteady-state conduction-heated foods. *Journal of Food Engineering*, 80(2), 581–593. <https://doi.org/10.1016/j.jfoodeng.2006.06.023>
- Dolan, K. D., & Mishra, D. K. (2013). Parameter estimation in food science. *Annual Review of Food Science and Technology*, 4, 401–422. <https://doi.org/10.1146/annurev-food-022811-101247>
- Dolan, K. D., Valdramidis, V. P., & Mishra, D. K. (2013). Parameter estimation for dynamic microbial inactivation: Which model, which precision? *Food Control*, 29(2), 401–408. <https://doi.org/10.1016/j.foodcont.2012.05.042>
- Dolan, K., Habtegebriel, H., Valdramidis, V. P., & Mishra, D. (2015). Thermal processing and kinetic modeling of inactivation. In: S. Bakalis, K. Knoerzer & P. J. Fryer (Eds.), *Modeling food processing operations* (pp. 37–66). Woodhead Publishing Series in Food Science, Technology and Nutrition.
- Donaldson, J. R., & Schnabel, R. B. (1987). Computational experience with confidence-regions and confidence-intervals for nonlinear least-squares. *Technometrics*, 29, 67–82. <https://doi.org/10.1080/00401706.1987.10488184>
- Draper, N., & Smith, H. (1981). *Applied regression analysis*. John Wiley & Sons.
- Enzweiler, H., Visioli, L. J., Muneron de Mello, J. M., Guelli Ulson de Souza, S. M. d. A., Ulson de Souza, A. A., Silva, A. d., Trigueros, D. E. G., & Schwaab, M. (2014). Statistical evaluation of biochemical kinetic models for BTX degradation. *Industrial & Engineering Chemistry Research*, 53(50), 19416–19425. <https://doi.org/10.1021/ie503408g>
- Efron B. (1979). Bootstrap methods: another look at the jackknife. *Annals of Statistics*, 7(1), 1–26.
- Fernández, A., Ocio, M. J., Fernández, P. S., Rodrigo, M., & Martínez, A. (1999). Application of nonlinear regression analysis to the estimation of kinetic parameters for two enterotoxigenic strains of *Bacillus cereus* spores. *Food Microbiology*, 16(6), 607–613. <https://doi.org/10.1006/fmic.1999.0282>
- Fernández, A., Ocio, M. J., Fernández, P. S., & Martínez, A. (2001). Effect of heat activation and inactivation conditions on germination and thermal resistance parameters of *Bacillus cereus* spores. *International Journal of Food Microbiology*, 63(3), 257–264. [https://doi.org/10.1016/S0168-1605\(00\)00454-2](https://doi.org/10.1016/S0168-1605(00)00454-2)
- Fleischman, G. J. (2015). Reducing the experimental effort in measuring *D* and *z* values for microorganism inactivation kinetics. *Journal of Food Engineering*, 155, 1–9. <https://doi.org/10.1016/j.jfoodeng.2014.12.023>
- Garre, A., Fernández, P. S., Lindqvist, R., & Egea, J. A. (2017). Bioinactivation: Software for modelling dynamic microbial inactivation. *Food Research International*, 93, 66–74. <https://doi.org/10.1016/j.foodres.2017.01.012>
- Garre, A., Clemente-Carazo, M., Fernández, P. S., Lindqvist, R., & Egea, J. A. (2018). Bioinactivation FE: A free web application for modelling isothermal and dynamic microbial inactivation. *Food Research International*, 112, 353–360. <https://doi.org/10.1016/j.foodres.2018.06.057>
- Giannakourou, M. C., & Stoforos, N. G. (2017). A theoretical analysis for assessing the variability of secondary model thermal inactivation kinetic parameters. *Foods*, 6(1), 7. <https://doi.org/10.3390/foods6010007>
- Gil, M. M., Brandão, T. R. S., & Silva, C. L. M. (2006). A modified Gompertz model to predict microbial inactivation under time-varying temperature conditions. *Journal of Food Engineering* 76(1), 89–94. <https://doi.org/10.1016/j.jfoodeng.2005.05.017>
- Goula, A. M., Prokopiou, P., & Stoforos, N. G. (2018). Thermal degradation kinetics of L-carnitine. *Journal of Food Engineering*, 231, 91–100. <https://doi.org/10.1016/j.jfoodeng.2018.03.011>
- Greiby, I., Mishra, D. K., Dolan, K. D., & Siddiq, M. (2017). Inverse method to estimate anthocyanin degradation kinetic parameters in cherry pomace during non-isothermal heating. *Journal of Food Engineering*, 198, 54–62. <https://doi.org/10.1016/j.jfoodeng.2016.11.005>
- Grijpspeerd, K. & De Reu, K. (2005). Practical application of dynamic temperature profiles to estimate the parameters of the square root model. *International Journal of Food Microbiology*, 101(1), 83–92. <https://doi.org/10.1016/j.ijfoodmicro.2004.10.042>
- Hayakawa, K., Schnell, P. G., & Kleyn, D. H. (1969). Estimating thermal death time characteristics of thermally vulnerable factors by programmed heating of sample solution or suspension. *Food Technology*, 23, 1090–1094.
- Haralampu, S. G., Saguy, I., & Karel, M. (1985). Estimation of Arrhenius model parameters using three least squares methods. *Journal of Food Processing and Preservation*, 9(3), 129–143. <https://doi.org/10.1111/j.1745-4549.1985.tb00715.x>
- He, L., Park, S. H., Hai Dang, N. D., Duong, H. X., Duong, T. P. C., Tran, P. L., Park, J. T., Ni, L., & Park, K. H. (2017). Characterization and thermal inactivation kinetics of highly thermostable ramie leaf β -amylase. *Enzyme and Microbial Technology*, 101, 17–23. <https://doi.org/10.1016/j.enzmictec.2017.02.011>
- Huang, L. (2009). Thermal inactivation of *Listeria monocytogenes* in ground beef under isothermal and dynamic temperature conditions. *Journal of Food Engineering* 90(3), 380–387. <https://doi.org/10.1016/j.jfoodeng.2008.07.011>
- Huang, L. (2013). Determination of thermal inactivation kinetics of *Listeria monocytogenes* in chicken meats by isothermal and dynamic methods. *Food Control*, 33(2), 484–488. <https://doi.org/10.1016/j.foodcont.2013.03.049>
- Huang, L. (2016). Evaluating the performance of a new model for predicting the growth of *Clostridium perfringens* in cooked, uncured

- meat and poultry products under isothermal, heating, and dynamically cooling conditions. *Journal of Food Science*, 81(7), M11754–M11765. <https://doi.org/10.1111/1750-3841.13356>
- Huang, L. (2020). Dynamic analysis of growth of *Salmonella* spp. in raw ground beef – Estimation of kinetic parameters, sensitivity analysis, and Markov Chain Monte Carlo simulation. *Food Control*, 108, 106845. <https://doi.org/10.1016/j.foodcont.2019.106845>
- Huang, L., & Li, C. (2020). Growth of *Clostridium perfringens* in cooked chicken during cooling: One-step dynamic inverse analysis, sensitivity analysis, and Markov Chain Monte Carlo simulation. *Food Microbiology*, 85, 103285. <https://doi.org/10.1016/j.fm.2019.103285>
- Huang, L., & Vinyard, B. T. (2016). Direct dynamic kinetic analysis and computer simulation of growth of *Clostridium perfringens* in cooked turkey during cooling. *Journal of Food Science*, 81(3), M692–M701. <https://doi.org/10.1111/1750-3841.13202>
- John, R. C. St., & Draper, N. R. (1975). D-optimality for regression designs: A review. *Technometrics*, 17(1), 15–23. <https://doi.org/10.2307/1267995>
- Johnson, M. L., & Frasier, S. G. (1985). Nonlinear least squares analysis. *Methods in Enzymology*, 117, 301–342. [https://doi.org/10.1016/S0076-6879\(85\)17018-7](https://doi.org/10.1016/S0076-6879(85)17018-7)
- Johnson, M. L., & Faunt, L. M. (1992). Parameter estimation by least-squares methods. *Methods Enzymology*, 210, 1–37. [https://doi.org/10.1016/0076-6879\(92\)10003-v](https://doi.org/10.1016/0076-6879(92)10003-v)
- Joshi, M., Seidel-Morgenstern, A., & Kremling, A. (2006). Exploiting the bootstrap method for quantifying parameter confidence intervals in dynamical systems. *Metabolic Engineering*, 8, 447–55. <https://doi.org/10.1016/j.ymben.2006.04.003>
- Juneja, V. K., Eblen, B. S., & Ramsom, G. (2001). Thermal inactivation of *Salmonella* spp. in chicken broth, beef, pork, turkey, and chicken: Determination of D- and z-values. *Journal of Food Science*, 66(1), 146–152. <https://doi.org/10.1111/j.1365-2621.2001.tb15597.x>
- Kubo, M. T. K., Rojas, M. L., Curet, S., Boillereaux, L., & Augusto, P. E. D. (2018). Peroxidase inactivation kinetics is affected by the addition of calcium chloride in fruit beverages. *LWT*, 89, 610–616. <https://doi.org/10.1016/j.lwt.2017.11.045>
- Leontidis, S., Fernandez, A., Rodrigo C., Fernandez, P. S., Magraner, L., & Martinez, A. (1999). Research note: Thermal inactivation kinetics of *Bacillus Stearothermophilus* spores using a linear temperature program. *Journal of Food Protection*, 62(8), 958–961. <https://doi.org/10.4315/0362-028X-62.8.958>
- Longhi, D. A., Martins, W. F., da Silva, N. B., Carciofi, B. A. M., de Aragão, G. M. F., & Laurindo, J. B. (2017). Optimal experimental design for improving the estimation of growth parameters of *Lactobacillus viridescens* from data under non-isothermal conditions. *International Journal of Food Microbiology*, 240, 57–62. <https://doi.org/10.1016/j.ijfoodmicro.2016.06.042>
- Luersen, M., & Le Riche, R. (2004). Globalized Nelder-Mead method for engineering optimization. *Computers & Structures*, 82(23–26), 2251–2260. <https://doi.org/10.1016/j.compstruc.2004.03.072>
- Lund, D. B. (1977). Design of thermal processes for maximizing nutrient retention. *Food Technology*, 31(2), 71–78.
- Mastwijk, H. C., Timmermans, R. A. H., & Van Boekel, M. A. J. S. (2017). The Gauss-Eyring model: A new thermodynamic model for biochemical and microbial inactivation kinetics. *Food Chemistry*, 237, 331–341. <https://doi.org/10.1016/j.foodchem.2017.05.070>
- Mishra, D. K., Dolan, K. D., & Yang, L. (2008). Confidence intervals for modeling anthocyanin retention in grape pomace during nonisothermal heating. *Journal of Food Science*, 73(1), E9–E15. <https://doi.org/10.1111/j.1750-3841.2007.00598.x>
- Motulsky, H. J., & Christopoulos A. (2004). *Fitting models to biological data using linear and nonlinear regression. A practical guide to curve fitting*. GraphPad Software Inc.
- Munack, A. (1989) Optimal feeding strategy for identification of Monod-type models by fed-batch experiments. In N. M. Fish, R. I. Fox, & N. F Thornhill (Eds.), *Computer applications in fermentation technology modelling and control of biotechnological processes* (pp. 195–204). Society of Chemical Industry by Elsevier Applied Science.
- Murphy, R. Y., Duncan, L. K., Beard, B. L., & Driscoll, K. H. (2003). D and z values of *Salmonella*, *Listeria innocua*, and *Listeria monocytogenes* in fully cooked poultry products. *Journal of Food Science*, 68(4), 1443–1447. <https://doi.org/10.1111/j.1365-2621.2003.tb09664.x>
- Nelder, J. A., & Mead, R. (1965). A simplex method for function minimization. *The Computer Journal*, 7(4), 308–313. <https://doi.org/10.1093/comjnl/8.1.27>
- Nunes, R. V., Rhim, J. W., & Swartzel, K. R. (1991). Kinetic parameter evaluation with linearly increasing temperature profiles: Integral methods. *Journal of Food Science*, 56(5), 1433–1437. <https://doi.org/10.1111/j.1365-2621.1991.tb04791.x>
- Peleg, M., Penchina, C. M., & Cole, M. B. (2001). Estimation of the survival curve of *Listeria monocytogenes* during non-isothermal heat treatments. *Food Research International*, 34(5), 383–388. [https://doi.org/10.1016/S0963-9969\(00\)00181-2](https://doi.org/10.1016/S0963-9969(00)00181-2)
- Peleg, M., Normand, M. D., & Corradini, M. G. (2005). Generating microbial survival curves during thermal processing in real time. *Journal of Applied Microbiology*, 98, 406–417. <https://doi.org/10.1111/j.1365-2672.2004.02487.x>
- Peleg, M., Normand, M. D., Corradini, M. G., Van Asselt, A. J., De Jong, P., & Ter Steeg, P. F. (2008). Estimating the heat resistance parameters of bacterial spores from their survival ratios at the end of UHT and other heat treatments. *Critical Reviews in Food Science and Nutrition*, 48(7), 634–648. <https://doi.org/10.1080/10408390701724371>
- Rhim, J. W., Nunes, R. V., Jones, V. A., & Swartzel, K. R. (1989a). Determination of kinetic parameters using linearly increasing temperature. *Journal of Food Science*, 54(2), 446–450. <https://doi.org/10.1111/j.1365-2621.1989.tb03103.x>
- Rhim, J. W., Nunes, R. V., Jones, V. A., & Swartzel, K. R. (1989b). A research note: Kinetics of color change of grape juice generated using linearly increasing temperature. *Journal of Food Science*, 54(3), 776–777. <https://doi.org/10.1111/j.1365-2621.1989.tb04710.x>
- Schwaab, M., & Pinto, J. C. (2007). Optimum reference temperature for reparameterization of the Arrhenius equation. Part 1: Problems involving one kinetic constant. *Chemical Engineering Science*, 62(10), 2750–2764. <https://doi.org/10.1016/j.ces.2007.02.020>
- Schwaab, M., & Pinto, J. C. (2008). Optimum reparameterization of power function models. *Chemical Engineering Science*, 63(18), 4631–4635. <https://doi.org/10.1016/j.ces.2008.07.005>
- Schwaab, M., Biscoia, J. E. C., Monteiro, J. L., & Pinto, J. C. (2008). Nonlinear parameter estimation through particle swarm optimization. *Chemical Engineering Science*, 63(6), 1542–1552. <https://doi.org/10.1016/j.ces.2007.11.024>

- Schwaab, M., Lemos, L. P., & Pinto, J. C. (2008). Optimum reference temperature for reparameterization of the Arrhenius equation. Part 2: Problems involving multiple reparameterizations. *Chemical Engineering Science*, 63(11), 2895–2906. <https://doi.org/10.1016/j.ces.2008.03.010>
- Timmermans, R. A. H., Mastwijk, H. C., Nierop Groot, M. N., & Van Boekel, M. A. J. S. (2017). Evaluation of the Gauss-Eyring model to predict thermal inactivation of micro-organisms at short holding times. *International Journal of Food Microbiology*, 263, 47–60. <https://doi.org/10.1016/j.ijfoodmicro.2017.10.001>
- Valdramidis, V. P., Geeraerd, A. H., Gaze, J. E., Kondjoyan, A., Boyd, A. R., Shaw, H. L., & Van Impe, J. F. (2006). Quantitative description of *Listeria monocytogenes* inactivation kinetics with temperature and water activity as the influencing factors; model prediction and methodological validation on dynamic data. *Journal of Food Engineering*, 76(1), 79–88. <https://doi.org/10.1016/j.jfoodeng.2005.05.025>
- Valdramidis, V. P., Geeraerd, A. H., Bernaerts, K., & Van Impe, J. F. M. (2008). Identification of non-linear microbial inactivation kinetics under dynamic conditions. *International Journal of Food Microbiology*, 128(1), 146–152. <https://doi.org/10.1016/j.ijfoodmicro.2008.06.036>
- Van Boekel, M. A. J. S. (1996). Statistical aspects of kinetic modeling for food science problems. *Journal of Food Science*, 61(3), 477–486. <https://doi.org/10.1111/j.1365-2621.1996.tb13138.x>
- Van Boekel, M. A. J. S. (2002). On the use of the Weibull model to describe thermal inactivation of microbial vegetative cells. *International Journal of Food Microbiology*, 74(1), 139–159. [https://doi.org/10.1016/S0168-1605\(01\)00742-5](https://doi.org/10.1016/S0168-1605(01)00742-5)
- Van Derlinden, E., Bernaerts, K., & Van Impe, J. F. (2008). Dynamics of *Escherichia coli* at elevated temperatures: effect of temperature history and medium. *Journal of Applied Microbiology*, 104(2), 438–453. <https://doi.org/10.1111/j.1365-2672.2007.03592.x>
- Van Derlinden, E., & Van Impe, J. F. (2010). Modeling microbial kinetics as a function of temperature: identification of the growth/inactivation interface. *IFAC Proceedings Volumes*, 43(6), 519–524. <https://doi.org/10.3182/20100707-3-BE-2012.0106>
- Van Derlinden, E., & Van Impe, J. F. (2012). Modeling microbial kinetics as a function of temperature: Evaluation of dynamic experiments to identify the growth/inactivation interface. *Journal of Food Engineering*, 108(1), 201–210. <https://doi.org/10.1016/j.jfoodeng.2011.03.037>
- Versyck, K. J., Bernaerts, K., Geeraerd, A. H., & Van Impe, J. F. (1999). Introducing optimal experimental design in predictive modeling: A motivating example. *International Journal of Food Microbiology*, 51(1), 39–51. [https://doi.org/10.1016/S0168-1605\(99\)00093-8](https://doi.org/10.1016/S0168-1605(99)00093-8)
- Versyck, K. J. E., Bernaerts, K., & Van Impe, J. F. M. (2000). Practical implementation of the optimal experiment design methodology for estimation of microbial heat resistance parameters. *IFAC Proceedings Volumes*, 33(15), 139–144. [https://doi.org/10.1016/S1474-6670\(17\)39740-9](https://doi.org/10.1016/S1474-6670(17)39740-9)
- Vieira, M. C., Teixeira, A. A., Silva, F. M., Gaspar, N., & Silva, C. L. M. (2002). *Alicyclobacillus acidoterrestris* spores as a target for Cupuaçu (*Theobroma grandiflorum*) nectar thermal processing: Kinetic parameters and experimental methods. *International Journal of Food Microbiology*, 77(1–2), 71–81. [https://doi.org/10.1016/S0168-1605\(02\)00043-0](https://doi.org/10.1016/S0168-1605(02)00043-0)
- Wang, X., Devlieghere, F., Geeraerd, A., & Uyttendaele, M. (2017). Thermal inactivation and sublethal injury kinetics of *Salmonella enterica* and *Listeria monocytogenes* in broth versus agar surface. *International Journal of Food Microbiology*, 243, 70–77. <https://doi.org/10.1016/j.ijfoodmicro.2016.12.008>

SUPPORTING INFORMATION

Additional supporting information may be found online in the Supporting Information section at the end of the article.

How to cite this article: Giannakourou M.C., Saltaouras K-P, Stoforos N.G. On optimum dynamic temperature profiles for thermal inactivation kinetics determination. *J Food Sci.* 2021;86:2172–2193. <https://doi.org/10.1111/1750-3841.15770>